공학박사학위논문

A Study of The SERS-based Decoding Strategy on Multiplex Suspension Array with Micro Beads

마이크로비드를 이용한 다중분석 서스펜션어레이에서
표면증강 라만분광법 기반 코드화에 관한 연구

2014년 2월

서울대학교 대학원
협동과정 의용생체공학전공
이 사 람

Ph.D. Dissertation

A Study of The SERS-based Decoding Strategy on Multiplex Suspension Array with Micro Beads

BY

SA RAM LEE

FEBRUARY 2014

INTERDISCIPLINARY PROGRAM FOR BIOMEDICAL ENGINEERING GRADUATE SCHOOL
SEOUL NATIONAL UNIVERSITY

ABSTRACT

A Study of The SERS-based Decoding Strategy on Multiplex Suspension Array with Micro Beads

Sa Ram Lee
Interdisciplinary Program for Biomedical Engineering
Graduate School
Seoul National University

This dissertation is focused on a barcoding strategy using Surface-enhanced Raman Scattering (SERS) for bead-based multiplex analysis. Barcoding or the indexing strategy for the probe particle is most important factor to quantify and classify the information for the suspension array assay. In this work, the author shows a practical implementation of the SERS decoding strategy for the suspension array assay that existed only in theory and explored the possibility of SERS as a barcoding strategy for a multiplex suspension array as

follow: i) consecutive SERS signal acquisition from micro beads moving in a microfluidic channel; ii) simultaneous detection of SERS and fluorescence signals from micro beads, and iii) fluorescence quantification and SERS decoding with micro beads for the suspension array.

First, the micro spherical gold beads were fabricated using electroless plating on PMMA beads and elegantly optimized to produce the effective SERS signals. The achieved beads produced well-defined SERS spectra even at an extremely short exposure time for a single bead combined with Raman tags such as 2-naphthalenethiol (2-NT) and benzenethiol (BT). The consecutive SERS spectra from a variety of combinations of Raman tags were successfully acquired from the beads at static and moving conditions. The proposed Raman tagged micro beads exhibited the potential of an on-chip microfluidic SERS decoding strategy for a micro suspension array.

Second, simultaneous detection of SERS and fluorescence signals using a single excitation source was shown with individually functionalized micro beads that can be applied to array-based multiplex analysis. The author chose proper beads that can produce well-defined SERS spectra and carefully engineered micro beads with a biomarker. The functionalized micro beads successfully worked

dependently, with not only the decoding function of the Raman tags but also with the probing function for analytes. Above all, author achieved simultaneous detection for SERS and fluorescence signals while avoiding signal overlapping between the two by carefully selecting the detection ranges.

Finally, based on the achieved technologies, the author demonstrates the flow cytometer that can measure fluorescence and SERS signals from a single micro bead in the flow. The flow cytometer includes pump controllable microfluidics and a customized Raman and fluorescence system and it can provide two pieces of independent information which is decoding results from the encoded Raman tags and quantifying the results from the fluorescence of the modified bead. Through this, the author shows that the SERS could be a useful decoding strategy for suspension arrays.

Keywords : Decoding strategy, Suspension array, Multiplex analysis, Micro spherical bead, Surface-enhanced Raman scattering (SERS), Fluorescence quantification, Flowing condition, Microfluidics system

Student Number : 2006-20800

CONTENTS

Abstract ····· i

Contents ····· iv

List of Figures ····· vii

Chapter 1. ····· 1

Introduction

1.1. Multiplex Array Assays ····· 2

1.1.1. Suspension Array and Planar Array ····· 2

1.1.2. Performance Comparison of Array Assays ····· 6

1.2. Barcoding Strategy for Suspension Assays ····· 9

1.2.1. Particle Encoding Technology ····· 9

1.2.2. SERS-based Strategy ····· 13

1.2.3. SERS Decoding for Multiplex Assays ····· 15

1.3. Goal of This Thesis ····· 18

Chapter 2. ····· 19

SERS Decoding of Micro Beads Moving in a Microfluidic Channel

2.1. Methods and Materials ····· 20
2.1.1. Preparation of Raman tagged Micro Beads ····· 20
2.1.2. Chip Fabrication and Channel Coating ····· 23
2.1.3. Instrumentation for SERS Measurements ····· 26
2.1.4. Experimental Set up ····· 28
2.2. Results and Discussion ····· 30
2.2.1. SERS from Static Micro Beads ····· 30
2.2.2. SERS from Moving Micro Beads in Microfluidic Channel 35
2.2.3. SERS Decoding of the Moving Micro Beads ····· 40

Chapter 3. ····· 42
Simultaneous Detection of SERS and Fluorescence Signals Using a Single Excitation Laser Source for Micro Bead-based Analysis
3.1. Methods and Materials ····· 43
3.1.1. Preparation of Functionalized Micro Beads ····· 43
3.1.2. Instrumentation for SERS and Fluorescence Measurements 46
3.2. Results and Discussion ····· 49
3.2.1. Antibody Response of the Functionalized Micro Beads ····· 49
3.2.2. Simultaneous Detection of SERS and Fluorescence ····· 52

Chapter 4. ····· 55

SERS Decoding and Fluorescence Quantification with Micro Beads for Suspension Array

4.1. Methods and Materials ····· 56

4.1.1. Preparation of Modified Micro Beads ····· 56

4.1.2. Chip fabrication and Microfluidic system ····· 61

4.1.3. Instrumentation for SERS and Fluorescence Measurements 64

4.2. Results and Discussion ····· 67

4.2.1. Optimized Flow Condition for SERS and Fluorescence in a Microfluidic Channel ····· 67

4.2.2. SERS Decoding and Fluorescence Quantification ····· 73

Chapter 5. ····· 75

Conclusion and Perspective

Bibliography ····· 79

국문초록 ····· 88

List of Figures

Figure 1-1. Schematic view of the suspension array. The suspension array composed of recognition agents attached to encoded beads. Recognition agents can be conjugated with a reagent specific to a particular bioassay such as antigens, antibodies, oligonucleotides, enzyme substrates or receptors. The identity of the recognition molecules attached to each particle is revealed by decoding the bead code. The suspension array has received great attention because of array preparation, sample volume, faster binding kinetics, lower costs, higher reproducibility, and superior detection sensitivity for multiplex analysis.

Figure 1-2. Schematic view of the planar array. A conventional planar array has elements or spots for a series of probe molecules on a two-dimensional plate with recognition agents such as DNA, antibodies, proteins, drug candidates, etc. The identity of the recognition agents at each spot in the array is known from its position in the plate.

Figure 1-3. A number of barcoding methods have been suggested for multiplex technologies. (a) photobleaching beads, (b) continuous-flow lithography based patterned-particles, (c) electrical method, (d) graphical rods, (e) quantum dots. Other barcoding techniques are also known such as metallic nanowires, shape based physical method, etc.

Figure 1-4. Representative Raman-based barcoding technology. (a) Encoding peptide sequences with surface-enhanced Raman spectroscopic nanoparticles. (b) DNA and RNA detection with nanoparticles using Raman spectroscopic fingerprints. (c) The encoding system based upon dispersible arrays of nanodisks prepared by on-wire lithography and functionalized with Raman active chromophores.

Figure 2-1. A micro spherical gold bead. (a) scanning electron microscope (SEM) image of the gold bead. (b) Schematic illustration of the Raman tagged micro gold bead for SERS measurement. The micro gold bead had a PMMA bead diameter of 15 μm at the core and an electrochemically roughened bead structure. The Raman tags were immobilized on the micro gold bead surface for the SERS measurements.

Figure 2-2. The microfluidic glass chip was fabricated by standard photolithography. The simple cross microfluidic channels were 75 μm wide and 25 μm deep. The microchannel walls were coated with a poly(diallyldimethylammoniumchloride) (PDADMAC) to prevent the adsorption of the micro gold beads.

Figure 2-3. Schematic view of the SERS instrumentations system. The SERS measurements were performed using a customized micro-Raman spectroscopic system equipped with a microscope.

Figure 2-4. Schematic illustration of the experimental set up and image of the microfluidic chip. (a) At static condition. (b) At fluidic condition.

Figure 2-5. Raman spectrum and schematic view of the surface modified gold bead with Raman tag. (a) BT spectra. (b) 2-NT spectra. (c) 2-NT/BT spectra.

Figure 2-6. The gold bead was reasonably capable of identifying the Raman tag from the spectra with an exposure time that was longer than 1 ms. (a) BT spectra. (b) 2-NT spectra.

Figure 2-7. SERS spectra of the micro gold beads tagged with

mixtures of 2-NT and BT with a series of molar ratios. The 2-NT and BT tags were responsible for the peaks at 1,370 cm^{-1} and 1,020 cm^{-1}, respectively. The relative heights of the peaks at 1,370 cm^{-1} and 1,020 cm^{-1} show the 2-NT:BT ratios of 0:1, 1:90, 1:10, 1:1 and 1:0, respectively. Acquisition time for the SERS measurements was 500 ms.

Figure 2-8. Consecutive SERS spectra of the encoded micro gold bead with Raman tags under the fluidic condition. (a), (b) and (c) are the consecutive SERS spectra from the Raman tags of 2-NT, BT and a mixture of 2-NT and BT (1:10), respectively.

Figure 2-9. Histogram of the characteristic peak ratios of the I_1 (1,020 cm^{-1}) / I_2 (1,370 cm^{-1}) from the SERS spectra in a microfluidic channel. (n = 10)

Figure 3-1. Schematic view of the functionalized micro spherical bead. The micro bead has 15 μm PMMA core where the antibody is conjugated with exposed amine groups and has silver nanoparticles on its surface where a Raman tag is chemisorbed (figures not drawn to scale).

Figure 3-2. Schematic illustrations of experimental set up. The

detectors for SERS and fluorescence signals are housed together in a single system. An emission filter (624 nm) is used to select fluorescence signals with PMT while SERS is detected through CCD.

Figure 3-3. Representative microscopy image of functionalized silver micro bead. (a) A light image. (b) A fluorescence image of sandwich immunoassay using 0.4 ng/ml cTnI cardiac marker proteins. Scale bars are 20 μm.

Figure 3-4. Control experiment to evaluate our immunoassay system. No fluorescence could be detected when (a) cTnI or (b) mouse anti-cTnI antibody was removed. (c) Fluorescence could be detected when all of the antigen-antibody response was completed.

Figure 3-5. Fluorescence (upper) and SERS (lower) signals from a single silver micro bead exactly coincide when simultaneously detected by laser scanning on a glass slide. The peak at 1,020 cm^{-1} was monitored as the representative SERS peak and fluorescence signals were filtered through a 624 ± 20 nm band pass filter.

Figure 4-1. Schematic view of the modified micro spherical bead. The micro bead has 15 μm PMMA bead core and

fluorescence molecule conjugated antibody is immobilized on its surface and the Raman tag is chemisorbed (figures not drawn to scale).

Figure 4-2. Evaluation of the enhancement factor of the micro bead. The enhancement factor can be as large as 1.4 x 10^6, theoretically.

Figure 4-3. (a) The microfluidic glass chip. It was fabricated by standard photolithography and is 85 μm wide and 25 μm depth. (b) The Microfluidic system. Bead delivery and sheath are provided by a pressure-driven flow with a syringe pump. For the connection to the pump, NanoPort Assemblies were equipped with a microfluidic chip.

Figure 4-4. An image of the experimental set up. Instrumentations include the Raman system, microfluidic chip, pump system, and data acquisition system.

Figure 4-5. Optimized flow condition. The change in bead velocity was detected by imaging CCD operated at 30 frames/second. In this experimental microfluidic system, the optimal pump setting was 30 μL/h.

Figure 4-6. Optimized condition for flowing bead control with pump system. Optimal flow rate to detect a reasonable SERS

signal from a single bead was 4 ~ 5 points/bead at a fixed data acquisition time.

Figure 4-7. Microscopic images of standard fluorescence micro bead. The standard fluorescence micro bead kit from bangs lab with an average diameter of 8.31 μm has five different fluorescence intensities (a) 0.23 %, (b) 1.01 %, (c) 4.60 %, (d) 21.88 %, (e) 100 %.

Figure 4-8. Performance evaluation of the fluorescence system. The emission wavelengths were measured at 520 nm by PMT. The results have a good linearity and reasonable error range (r^2= 0.9886).

Figure 4-9. (a) Histograms of the number of events plotted against the magnitude of the fluorescence from three different modified beads. (b) Scatter plot of the modified beads delineated by particle transit time against the magnitude of the fluorescence of the modified beads. The bead population is clearly delineated.

Chapter 1.

Introduction

1. Introduction

1.1. Multiplex Array Assays

1.1.1. Suspension Array and Planar Array

In the 21st century, collection of integrated molecule information about genes, proteins, and other biomolecule is a major goal for biomedical research. New technologies have enabled the rapid acceleration of data collection and interpretation. Continued progress toward transforming this information into biomedical understanding is dependent on continued improvement in analytical technologies. In particular, it is critical to augment qualitative analysis methods that enable the collection of important quantitative information. Furthermore, the rapid advance in biochemical studies, clinical diagnostics, drug screening and environmental monitoring keeps stimulating the demand for powerful analytical methods to collect a huge amount of information [1-6].

In general, large-scale analysis technologies can be categorized into two strategies: the assay chemistry and the detection platform - planar array and suspension array (using encoded particles). A planar array, which has elements or spots as a series of

probe molecules on a chip surface, is suitable for high-density analysis such as DNA and protein microarrays. The big advantage of all these approaches is that the position or location of a spot on the microarray acts as an address for identification, and hence, the reaction products are known. However, with fixed reagent spots, analytes will require additional time to find their complementary spot (hybridization times of several hours or more). This is because assays often depend solely on the diffusion of analytes to the surface-bound probes. The suspension array is emerging as a multiplexing technology and an alternative to the planar array [3-5].

Conceptually, suspension arrays are similar to a planar array, with distinct quanta for an optical parameter which act as a substitute for the physical location on a surface. Beyond this similarity, multiplex analysis using a suspension array differs significantly in its implementation and offers many valuable advantages over the planar array in terms of array preparation, sample volume, faster binding kinetics, lower costs, higher reproducibility, and superior detection sensitivity.

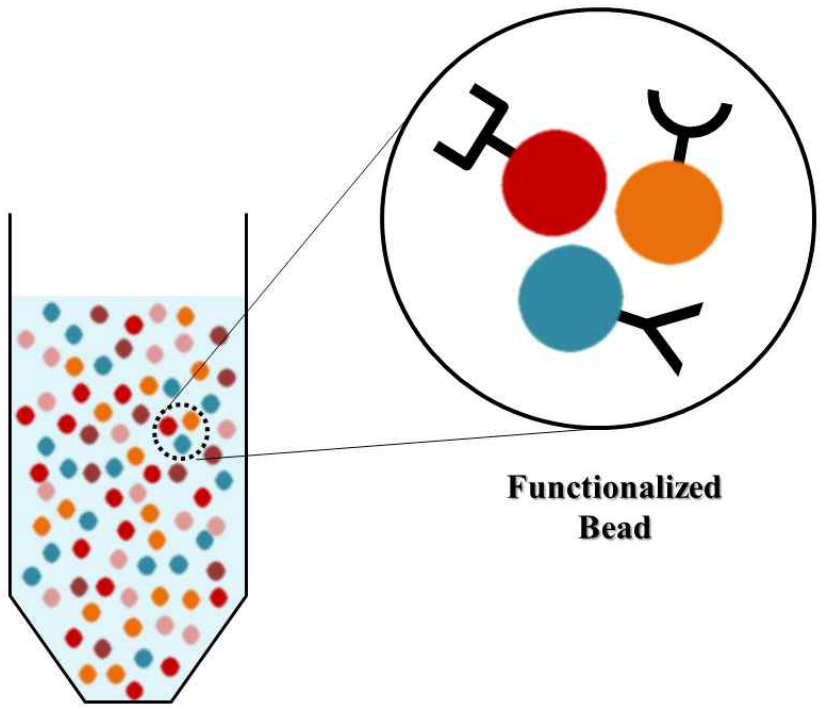

Figure 1-1. Schematic view of the suspension array. The suspension array composed of recognition agents attached to encoded beads. Recognition agents can be conjugated with a reagent specific to a particular bioassay such as antigens, antibodies, oligonucleotides, enzyme substrates or receptors. The identity of the recognition molecules attached to each particle is revealed by decoding the bead code. The suspension array has received great attention because of array preparation, sample volume, faster binding kinetics, lower costs, higher reproducibility, and superior detection sensitivity for multiplex analysis.

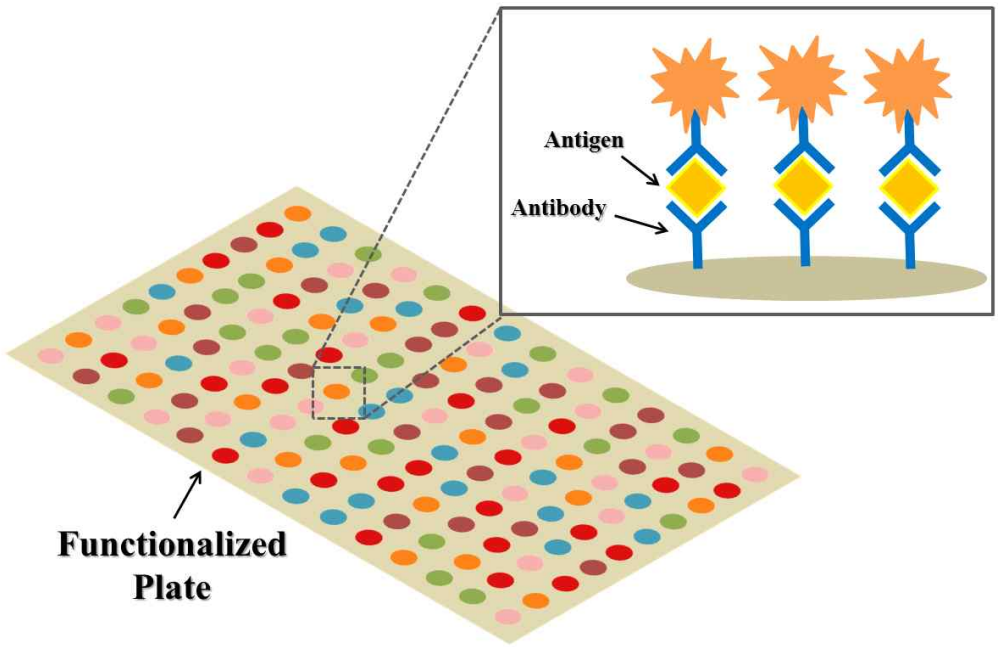

Figure 1-2. Schematic view of the planar array. A conventional planar array has elements or spots for a series of probe molecules on a two-dimensional plate with recognition agents such as DNA, antibodies, proteins, drug candidates, etc. The identity of the recognition agents at each spot in the array is known from its position in the plate.

1.1.2. Performance Comparison of Array Assays

In each planar array, each array spot is prepared individually, using spotting robots or photolithography. Although it is possible to attain multiple arrays in parallel simultaneously, there is a limit to the number of array spots that can be prepared at one time. In suspension arrays, however, each array element is prepared in bulk. A suspension of beads typically contains tens of millions of particles per milliliter that, when coupled with the appropriate receptor such as an antibody, protein, nucleic acid, or molecule can be used to prepare thousands of microsphere arrays. The use of beads in analyses may have even better yield results between analytes and receptors. This is because the available binding surface area per unit volume may be significantly increased. It becomes possible to carry out effective reactions with suspension array in much smaller volumes. Thus, suspension arrays can effectively act to amplify signals as results. In addition, if the beads can be moved through solution using some kind of agitation such as electric fields, magnetic fields, pressure-driven flow, gravity, etc. Mass transport to the receptor surface is no longer a limiting factor in suspension array, and the binding kinetics and thermodynamics are improved. This in turn means improved analysis times [2, 4, 5, 7, 8].

Along the same line, the results published to date have compared data from suspension arrays and planar arrays: ELISA (Enzyme-Linked Immuno Specific Assay) which is widely accepted as the current 'gold standard' [9-13]. Although, the degree of correlation has varied widely because of the methods on how these comparisons were made as well as the antibodies used in each of the assays, many of the published researches have reported good correlations between suspension arrays and ELISAs [10-13]. Among them, Ray and colleagues carefully examined with a large study of more than 2000 serum samples the validation and implementation of cytokine multiplex assays, as a replacement for ELISA. Although a fairly good correlation was found between these assays, the multiplex results were, on average, 2.36 times higher than the ELISA results [9, 13]. Even though researchers point to differences in antibody pairs, sample diluents, pH and salt concentrations as likely causes of the observed differences when comparing two strategies, given the fact that suspension arrays are cost- and time-effective, and minimize the sample volume requirements, bead-based array assays are likely to become increasingly commonplace .

As a result, the spectrum of suspension arrays is enormously broad, and includes immunoassay, affinity assay, DNA hybridization assay, and protein - DNA, protein - protein, and enzymological studies.

The clinical diagnostics, high-throughput screening, and combinatorial chemistry fields have all benefited.

1.2. Barcoding Strategy for Suspension Assays

1.2.1. Particle Encoding Technology

The suspension array for multiplex analysis and its operation in microfluidic systems definitely requires reliable and efficient decoding as well as encoding. The desirable encoding strategy should reproducibly create as many stable libraries as possible using a simple process. In order to do so, the process must not involve any complicated synthetic steps and must be insensitive to the reaction conditions. It should not need sophisticated tuned-complex optics or leave any residual chemicals. The ideal decoding on a microfluidic chip should allow for quick, non-destructive, non-invasive, and reliable identification during the process in a microfluidic network. To meet these conditions, a number of encoding and decoding methods have been suggested for multiplex technologies [14-16], e.g. fluorescence [17-21], quantum dots [22-24], graphical rods [25, 26], photobleaching beads [27], continuous-flow lithography based particles [28], a physical method [29, 30], and an electrical method [31]. Despite these suggestions and demonstrations, better barcoding methods are still required.

The most well-known commercialized bead technology is

xMAP. The xMAP (Multi-Analyte Profiling) technology, licensed from Luminex Corp., employs 5.6 μm polystyrene microspheres that are internally dyed with two spectrally distinct fluorophores. This technique has 100 (up to 500) color encoded microsphere sets created with two fluorescent dyes at distinct ratios. A specific probe for a particular bioassay such as antigens, antibodies, oligonucleotides, enzyme substrates or receptors are conjugated to the surfaces of the microspheres. The microspheres when the reaction is completed are drawn into the array reader and probed individually in a rapidly flowing fluidic stream, in which a light source such as a laser or LED excites the beads individually. Generally, the red wavelength light excites the fluorescence in each bead, identifying its address and the green wavelength light excites the reporter molecule associated with the quantification of the captured analytes. High-speed signal processors and software record and classify the information based on its spectral address and quantify the reaction on the surface [9, 32-34]. This xMAP technology is available to partner companies, who in turn use this technology to develop commercial bead-based assay reagent kits for sale to consumers. Therefore, many applications with xMAP technology have reported cytokine quantitation [35], hormonal analysis [36], single nucleotide polymorphism genotyping [37], growth factors [38], and characterization of molecular interactions of nuclear

receptors [39]. Luminex® Corporation released the first flow cytometer designed specifically for multiplexed micro bead analysis in the late 1990s. Today, multiplexing analysis solutions such as MAGPIX, Luminex 100/200, and FLEXMAP 3D are commercially available. Bio-Rad Corporation supplies the similar product named Bio-Plex.

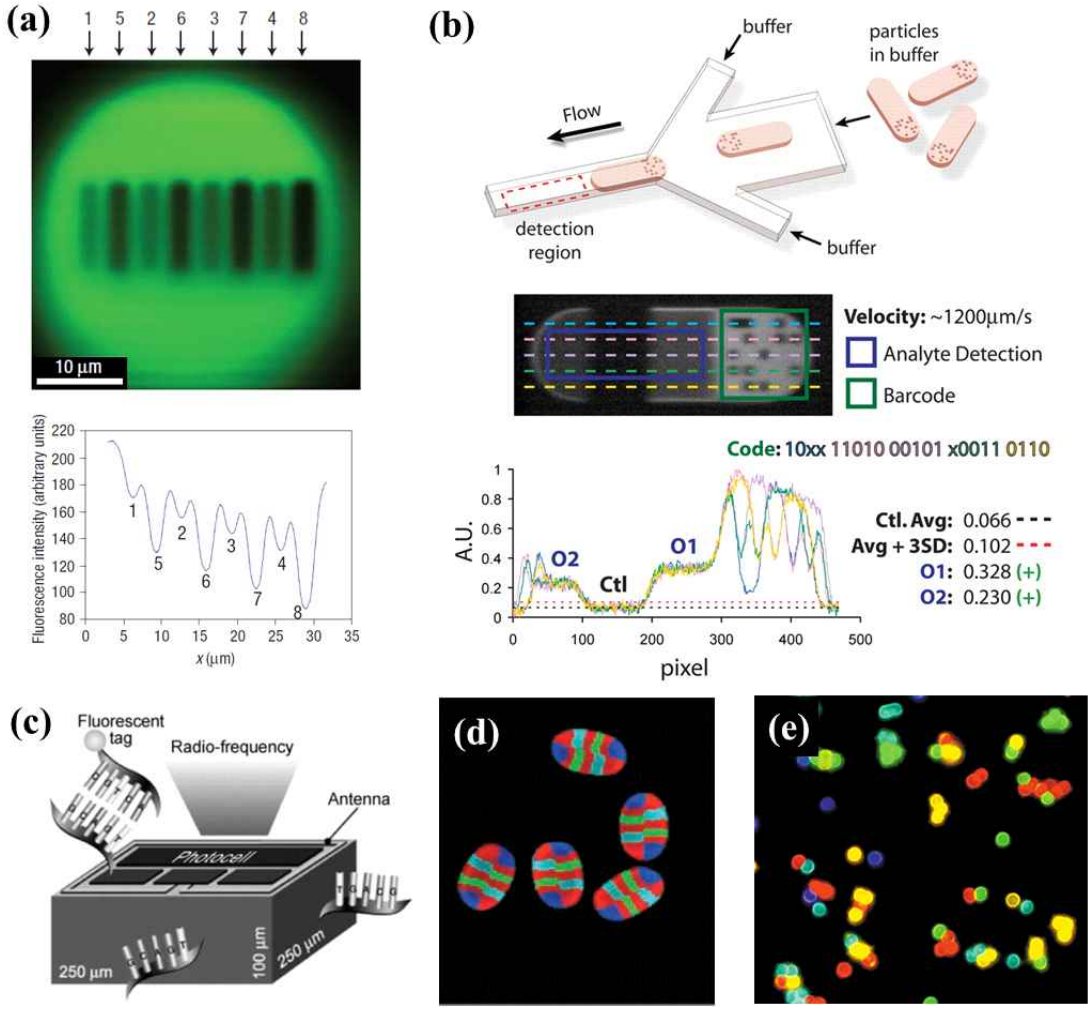

Figure 1-3. A number of barcoding methods have been suggested for multiplex technologies. (a) photobleaching beads, (b) continuous-flow lithography based patterned-particles, (c) electrical method, (d) graphical rods, (e) quantum dots. Other barcoding techniques are also known such as metallic nanowires, shape based physical method, etc.

1.2.2. SERS-based Strategy

Although fluorescence is principally employed in multiplex detection methods because of its high sensitivity compared with other signal sources, it has inherent drawbacks, including a broad emission band, photobleaching, and peak overlapping and thus, has a limited number of barcodes. Recently, surface-enhanced Raman spectroscopy (SERS) has received a great deal of attention as a promising analysis strategy [40-55]. SERS is a powerful vibrational spectroscopy technique that allows for highly sensitive structural detection of low concentration analytes through the amplification of electromagnetic fields generated by the excitation of localized surface plasmons [46, 56]. SERS employs smaller tags than any of the other barcoding methods that have been previously reported. Unlike most of the molecular spectroscopic techniques, Raman spectroscopy offers chemical identification in aqueous solutions without degradation concerns such as photobleaching, etc. SERS is also advantageous because of its narrow signal band and non-destructive detection [41, 42, 46, 57, 58]. As light sources and monochromatic devices are rapidly becoming miniaturized, the entire system for Raman spectroscopic detection is now portable and thus available even for field tests [59]. A key challenge in the Raman spectroscopic technique

for rapid detection, which is essential for high-throughput decoding on microfluidic chips, is its weak signal strength. In regard to this issue, SERS-active substrates have been improved over the last decade to enhance the conventional Raman signals by 6 ~ 10 orders of magnitude. Several SERS-active substrates have been formed based on nanosphere lithography [60], nanodisk [61], electrodeposited metal surfaces [62], tip-enhanced Raman scattering (TERS) [63] and nanowire bundles [64]. Among the previous suggestions, nanobeads consisting of a dielectric core with a thin gold coating are noticeable in terms of their potential for individual SERS probes [65].

1.2.3. SERS Decoding for Multiplex Assays

Concerning SERS decoding, a few groups have reported a Raman tag labelling strategy using micro-sized beads for DNA and protein detection [49, 52, 53, 66-72]. Cao et al. suggested that the Raman intensities at a single Raman shift can be used for DNA and RNA detection [66]. The relative SERS intensities were proven to be useful for the spectroscopic decoding strategy and improved in order to be implemented with mixed SAM on a gold surface [68, 73]. A chemically encoded organic-inorganic nanoparticles (COINs) system was developed by Su et al. for multiplex detection [67]. Jun et al. demonstrated multiplex immunoassays using SERS encoded beads for p53 antibody-antigen and biotin-streptavidin interactions [69]. Very recently, SERS-fluorescence joint spectral encoding method was demonstrated by Zhuyuan Wang. By conjugating different antibodies to organic-metal-quantum dot hybrid nanoparticles with varied codes, barcoding strategy has been studied by multiplex sandwich immunoassays [53]. Unfortunately, these reported technologies were suitable for a planar array rather than a suspension array.

Because of the narrow spectral band of SERS compared to fluorescent labels making possible multiparameter measurements, a combination system of flow cytometry and Raman measurements has

been gaining attention. The several groups demonstrated the possibility of addressing individual nanoparticles with SERS in a flow system several times [51, 74-76]. Cecchini et al. showed a droplet-based microfluidic system with ultrafast SERS detection and asserted that their approach allows for high-throughput analysis for a biological assay or molecular interactions [77]. However, most flow-based SERS studies adopted nanoparticles that not only are impossible to signal from a single particle or probe but are also hard to control in a fluidic system. And nanoparticles are too small and produce signals that are too weak to be applied to *in situ* decoding on microfluidic chips. These limitations of current systems demonstrate the necessity for a brand new feasible SERS decoding strategy for suspension arrays.

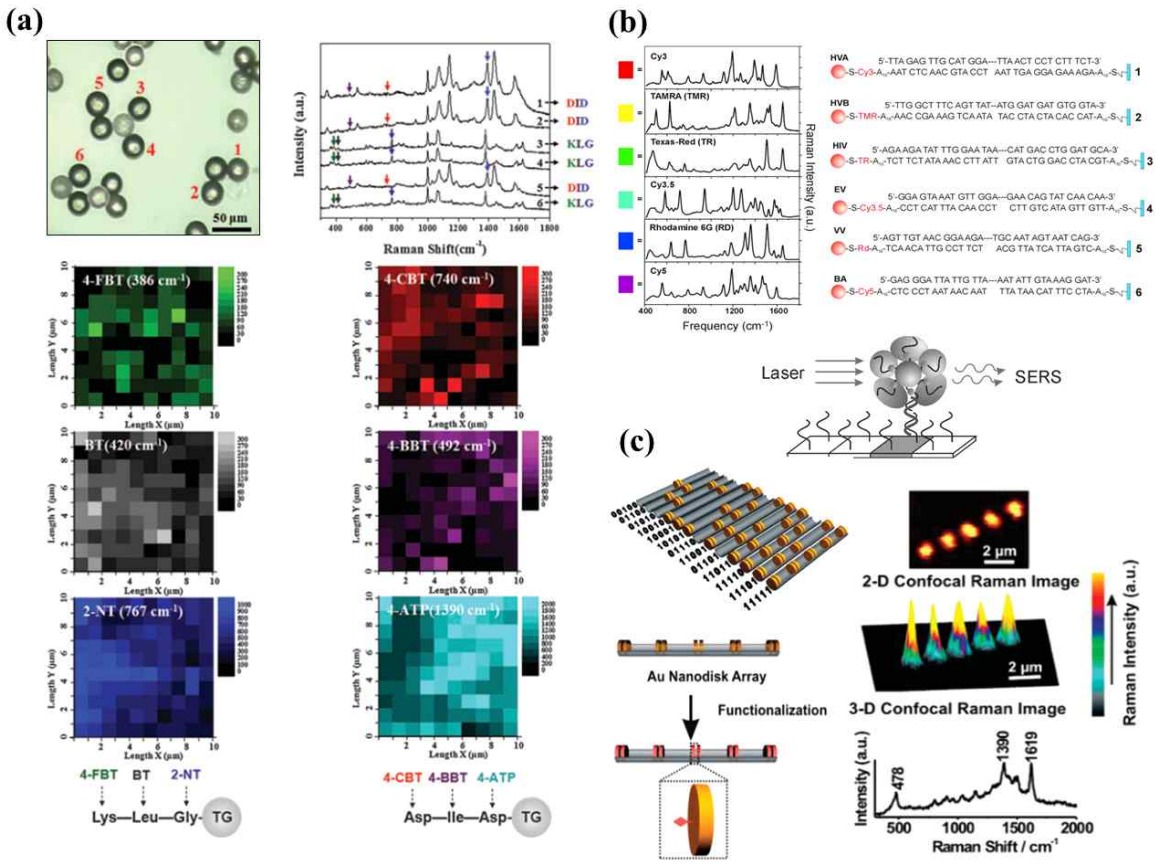

Figure 1-4. Representative Raman based barcoding technology. (a) Encoding peptide sequences with surface-enhanced Raman spectroscopic nanoparticles. (b) DNA and RNA detection with nanoparticles using Raman spectroscopic fingerprints. (c) The encoding system based upon dispersible arrays of nanodisks prepared by on-wire lithography and functionalized with Raman active chromophores.

1.5. Goal of This Thesis

In the 21st century, with the rapid advancement of biomedical research, the suspension array, which is a bead-based analytical methodology, has received great attention because of its array preparation, sample volume, faster binding kinetics, lower costs, higher reproducibility, and superior detection sensitivity. Additionally, suspension arrays are expected to provide us with effective opportunities to collect huge amounts of information for biochemical studies, clinical diagnostics, and drug screening. Therefore, having a stable and promising barcode or index strategy for the probe particle is the most important factor to classify information from a suspension array assay.

The ultimate goal of this study was to demonstrate the SERS decoding strategy for bead-based multiplex analysis. In this work, the author explored the possibility of using SERS as a barcoding strategy for suspension arrays and showed i) consecutive SERS signal acquisition from micro spherical beads moving in microfluidic chip, ii) simultaneous detection of SERS and fluorescence signals from micro spherical beads and iii) fluorescence quantification and SERS decoding with micro beads for suspension arrays.

Chapter 2.

SERS Decoding of Micro Beads Moving in a Microfluidic Channel

2.1. Methods and Materials

2.1.1. Preparation of Raman tagged Micro Beads

The micro gold beads were fabricated using an electroless plating method. Briefly, colloidal gold nanoparticles (AuNPs, 2 to 3 nm in diameter) were synthesized as previously described [50, 78] and attached to amine-terminated PMMA beads (PMMA-NH_2, 15 μm in diameter, Bangs Laboratories, Inc.) as seed layers. In this study, relatively bigger size beads were chosen, because they make it easier for laser focusing and controlling SERS decoding for the fluidic experiment condition. For the roughened bead structure from the AuNP seed, an Au plating solution comprised of $HAuCl_4$ and reducing agents (i.e., formaldehyde and hydroxylamine) were added to the PMMA-NH_2/AuNP solution, with vigorous stirring. After all the $HAuCl_4$ was reduced, the solution was centrifuged at 2,000 rpm for 5 min. The rinsing process was repeated several times with deionized (DI) water by centrifuging and decanting the supernatant. The amounts of added $HAuCl_4$ were adjusted to control the surface topology of the micro gold beads, and the optimal Au loading level was determined by SERS measurements. In this work, 1 mM 2-naphthalenethiol (2-NT, Sigma-Aldrich), 10 mM benzenethiol (BT,

Sigma-Aldrich), and mixture of 2-NT and BT (1:1, 1:10 and 1:90 molar ratios) were employed as Raman tags to functionalize the gold micro beads. The Raman tags were dissolved in ethanol to make 1 ml solutions, and the beads were immersed in the solutions for 24 h at 4 °C. The functionalized micro gold beads were centrifuged and washed with DI water several times to remove the excess reagents. Then, the Raman tagged micro gold beads were dispersed in DI water for storage before use. **Figure 2-1** illustrates the structure of the Raman tagged micro gold beads.

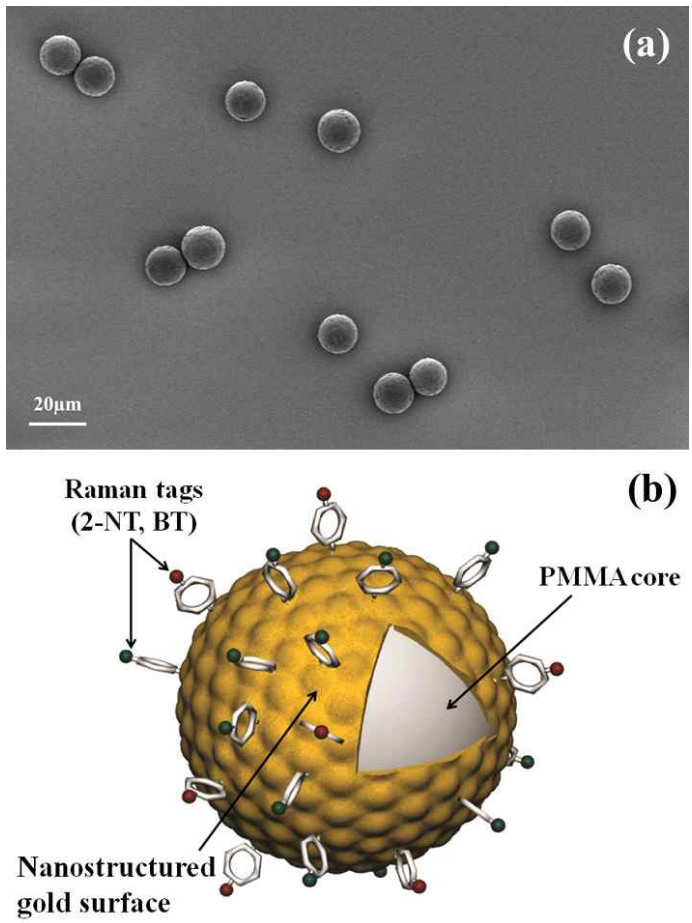

Figure 2-1. A micro spherical gold bead. (a) scanning electron microscope (SEM) image of the gold bead. (b) Schematic illustration of the Raman tagged micro gold bead for SERS measurement. The micro gold bead had a PMMA bead diameter of 15 μm at the core and an electrochemically roughened bead structure. The Raman tags were immobilized on the micro gold bead surface for the SERS measurements.

2.1.2. Chip Fabrication and Channel Coating

A slide glass (Corning, NY, USA) was cleaned in a piranha solution (H_2SO_4 : H_2O = 3:1) for 30 min and then baked on a hot plate for dehydration at 150 °C for 3 min. In order to enhance the adhesion between the glass substrate and the photoresist (PR), hexamethyldisilazane (HMDS) (J.T. Baker, USA) was spin coated onto the glass substrate at 6,000 rpm for 30 s (SC-102, Won Corporation, Korea). The slide glass was then baked on a hot plate at 150 °C for 90 s and cooled to room temperature. The PR (AZ4620, Clariant, Switzerland) was spin coated at 6,000 rpm for 30 s and then soft baked on a hot plate at 100 °C for 90 s. Then the soft baked slide glass was exposed to ultraviolet (UV) light at 365 nm at a dose of 180 m J cm^{-2} under a photo mask with a mask aligner (MDA-400M, MIDAS system, Korea). The UV exposed PR was developed using a developer (AZ400K, Clariant), and the patterned substrate was hardened by baking it on a hot plate at 150 °C for 15 min to increase the tolerance of the PR to the glass etching solution. With the other side of the slide glass protected, the microchannels were etched with buffered hydrofluoric acid (NH_4F:HF = 6:1, J.T. Baker) for 40 min at room temperature. The chip was sequentially rinsed with DI water and piranha solution and then sonicated. Holes

were drilled as reservoirs on another flat slide glass, and then the etched and drilled slide glasses were bonded thermally in a melting furnace (CRF-M15, CEBER, Korea) for 24 h [79-81]. The microchannel walls were modified with a polyelectrolyte multilayer using a procedure previously described in the literature to precisely control the electrokinetic flow and to prevent the adsorption of the functionalized micro gold beads. Poly(diallyldimethylammoniumchloride) (PDADMAC, Aldrich, Mw = 100,000 - 200,000), which does not give any appreciable Raman scattering peaks, was used as the cationic coating material. Initially, all of the channels were rinsed with 0.1 M NaOH for 10 min and deionized (DI) water, sequentially, for 10 min. Then 5 wt.% PDADMAC (monomer concentration) flowed through the channels for 10 min, and the channels were rinsed with DI water for 5 min to remove the residual PDADMAC. **Figure 2-2** shows the microfluidic chip used for these tests.

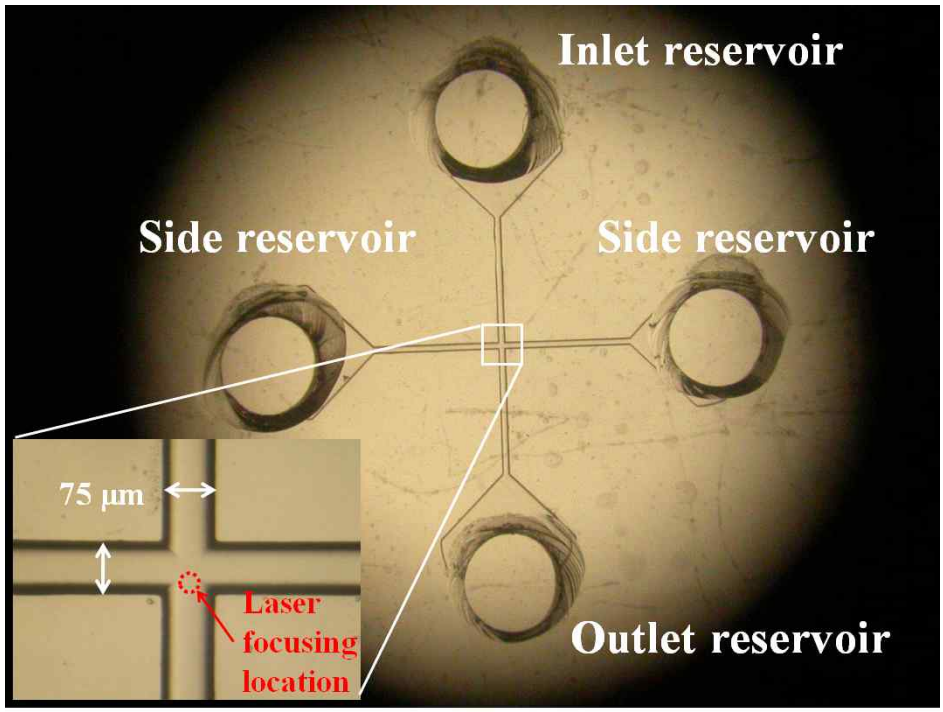

Figure 2-2. The microfluidic glass chip was fabricated by standard photolithography. The simple cross microfluidic channels were 75 μm wide and 25 μm deep. The microchannel walls were coated with a poly(diallyldimethylammoniumchloride) (PDADMAC) to prevent the adsorption of the micro gold beads.

2.1.3. Instrumentation for SERS Measurements

The SERS measurements were performed with a customized Ramboss micro-Raman spectroscopic system equipped with a microscope. The excitation source was a HeNe laser (633 nm, LASOS Lasertechnik GmbH, US) with an output power of 20 mW and a beam diameter of 2 μm. The laser beam was focused through a 100 X objective lens. The Raman scattering was detected with a TE cooled (-50 °C) charge coupled device (CCD) camera (1,024 X 127 pixels, Andor, iDus DV401). The calibration of the spectrometer was achieved with the Raman band of a silicon wafer at 520 cm^{-1} to normalize the peak intensities of the Raman tags on the micro gold beads. **Figure 2-3** shows a simple schematic view of the Instrumentation system for the SERS measurement.

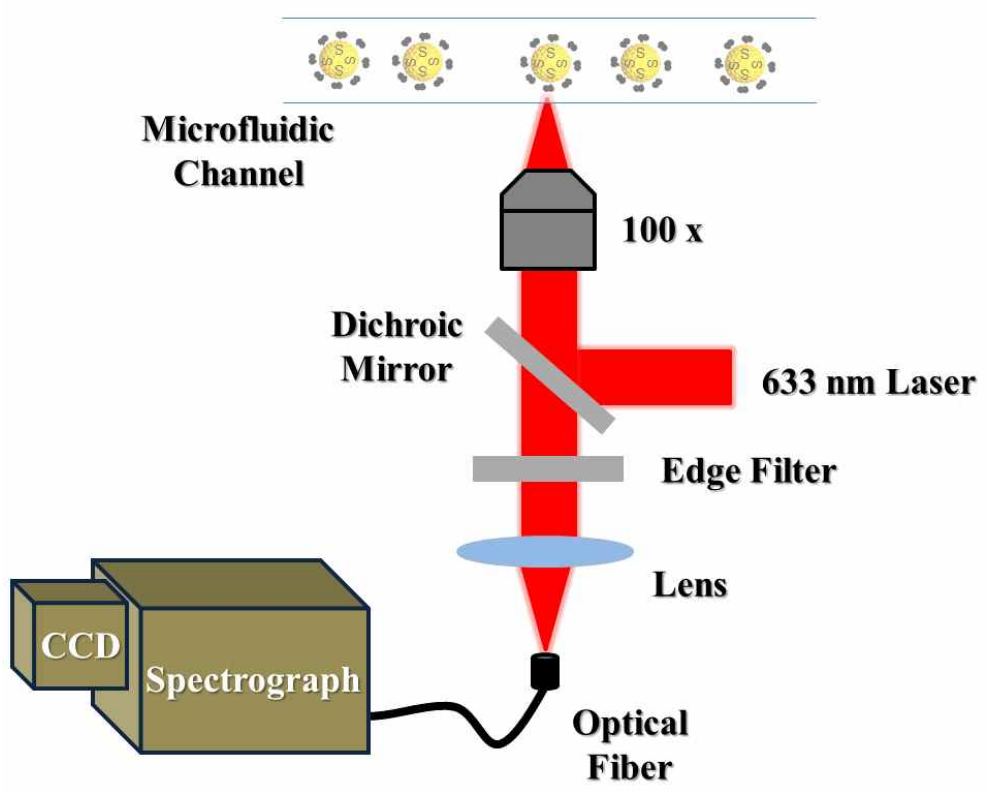

Figure 2-3. Schematic view of the SERS instrumentations system. The SERS measurements were performed using a customized micro-Raman spectroscopic system equipped with a microscope.

2.1.4. Experimental Set up

Figure 2-4 shows the SERS decoding method used in this work. The SERS signals from the functionalized micro gold beads were decoded under two different situations. **Figure 2-4 (a)** is a schematic view that shows the SERS decoding from the functionalized micro gold beads placed on a slide glass substrate. After dropping the functionalized micro gold beads on the slide glass, a laser beam was focused on the center of the gold bead, and the SERS spectra were obtained as a function of the acquisition time. **Figure 2-4 (b)** depicts the SERS decoding method carried out with the micro gold beads flowing in a microfluidic channel. The functionalized micro gold beads were dispersed in a 3 wt.% PDADMAC solution and placed into the reservoirs. The hydraulic pressure, induced by the level difference between the inlet and outlet reservoir, drove the micro gold beads through the microfluidic channel. For a stable hydraulic pressure, the level of the reservoirs was monitored during the fluidic experiments. The flow was hydrodynamically focused with two sheath flows to reduce the coincident effect and to make the micro gold beads reproducibly pass the laser spot. The laser beam was focused around the center of the junction area where the two channels crossed. The SERS measurements were consecutively conducted every 500 ms for 150 s.

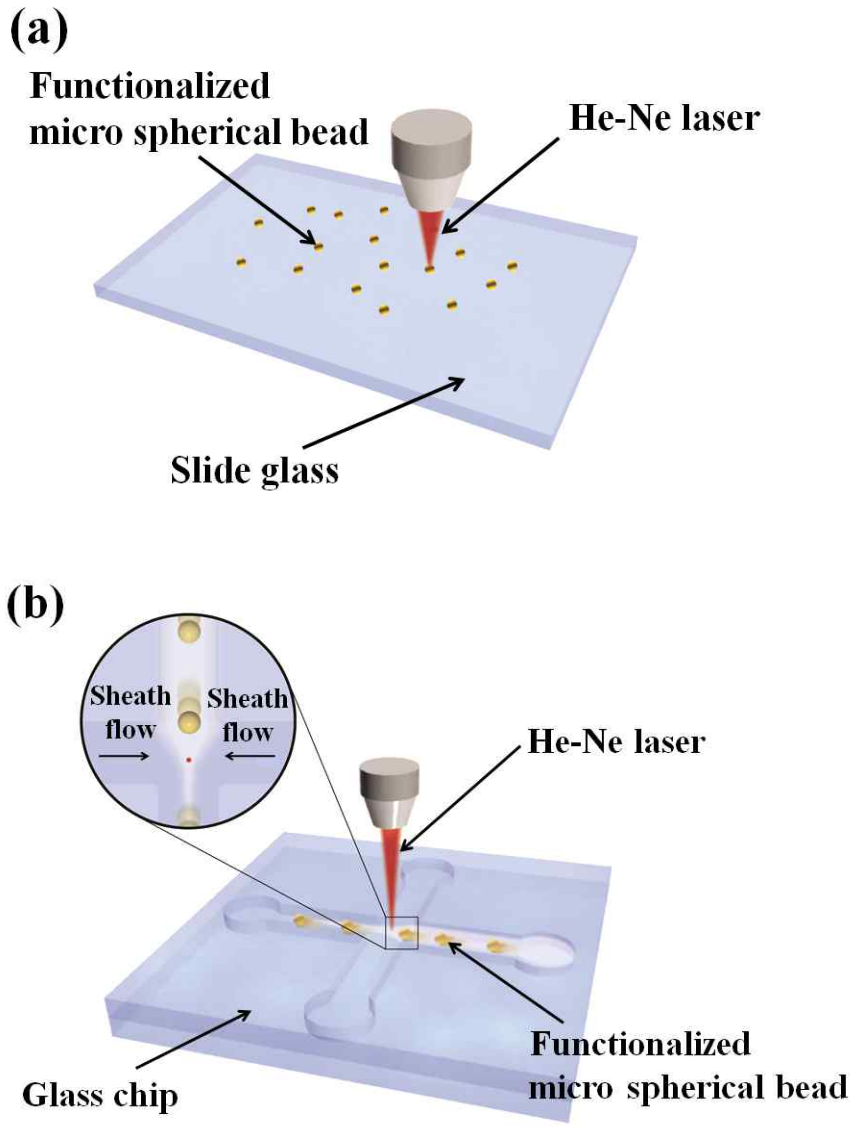

Figure 2-4. Schematic illustration of the experimental set up and image of the microfluidic chip. (a) At static condition. (b) At fluidic condition.

2.2. Results and Discussion

2.2.1. SERS from Static Micro Beads

Prior to the experiments in the microfluidic chips, the signals of various combinations of Raman tags were optimized with the micro gold beads immobilized on a glass slide, which was easily recognized through an optical microscope with a 100 X objective lens. **Figure 2-5** shows the Raman fingerprint of three Raman tags used to modify the surface of the gold beads. The elegantly tailored surfaces of the micro gold beads exhibited spectra containing well-defined peaks that were used to identify both of the Raman tags BT and 2-NT with exposure times longer than 1 ms (**Figure 2-6**). **Figure 2-7** shows the SERS spectra of the micro gold beads functionalized with two different Raman tags with a variety of fractional ratios on the slide glass. The 2-NT and BT Raman tags and the 2-NT/BT mixture, which were chemisorbed onto the micro gold bead surfaces, were clearly identified from the characteristic peaks in the SERS spectra. The 2-NT and BT tags were responsible for the peaks at 1,370 cm^{-1} and 1,020 cm^{-1}, respectively. The results showed that the molecular barcodes encoded on the micro gold beads produced intense and reproducible SERS spectra. Although the

absolute intensities of the peaks in the SERS spectra varied significantly, the relative intensities were unchanged and reliably reflected the ratio of the mixture of Raman tags on the micro gold bead surface. Repetitive measurements with a single micro gold bead and independent tests with many micro gold beads confirmed that the relative intensities of the characteristic peaks were highly reproducible. Consequently, the high sensitivity and the constant relative intensities of the SERS signals suggested the presence of a number of barcode libraries with conventional Raman tags. These results were consistent with a previous report by Jin et al [68].

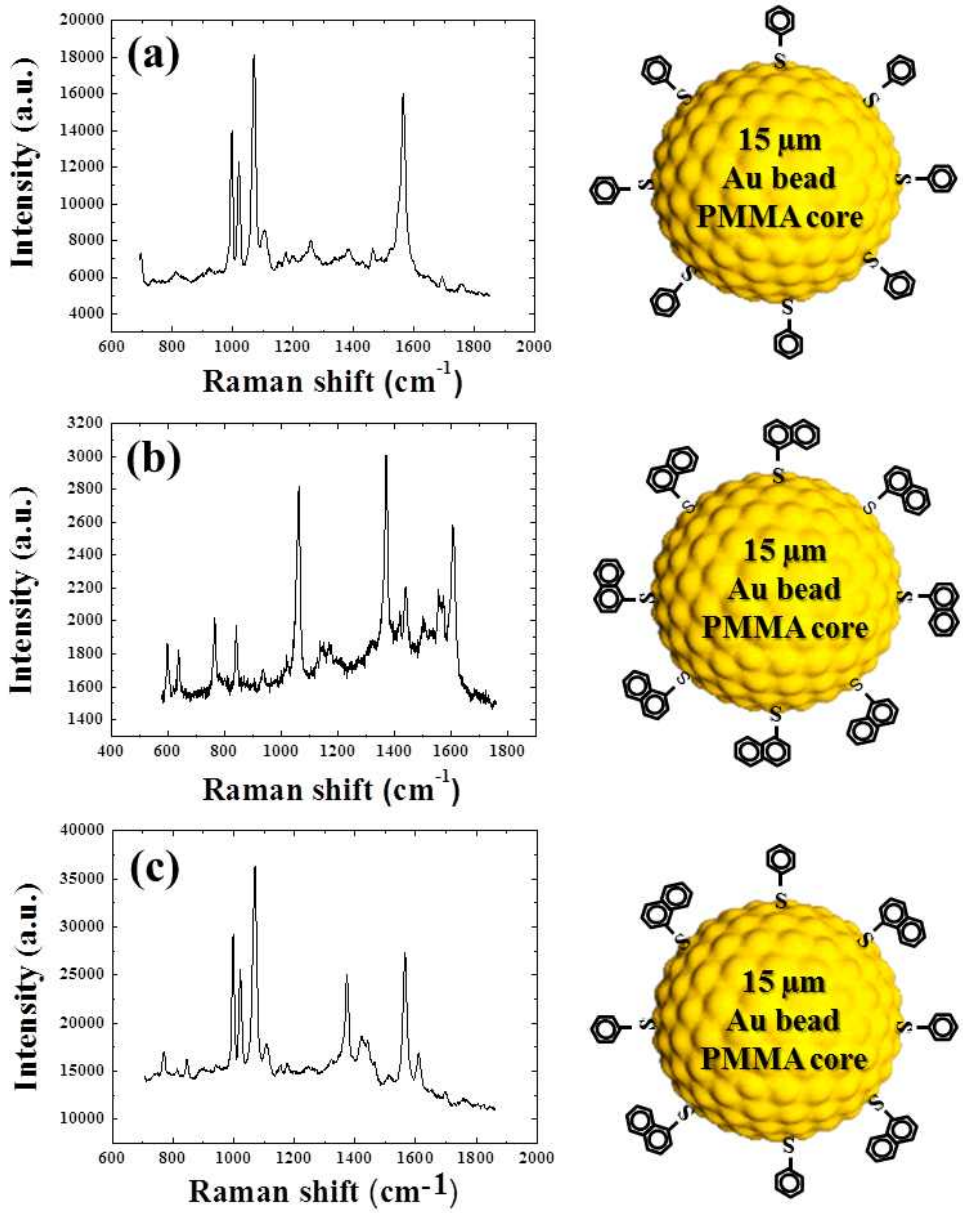

Figure 2-5. Raman spectrum and schematic view of the surface modified gold bead with Raman tag. (a) BT spectra. (b) 2-NT spectra. (c) 2-NT/BT spectra.

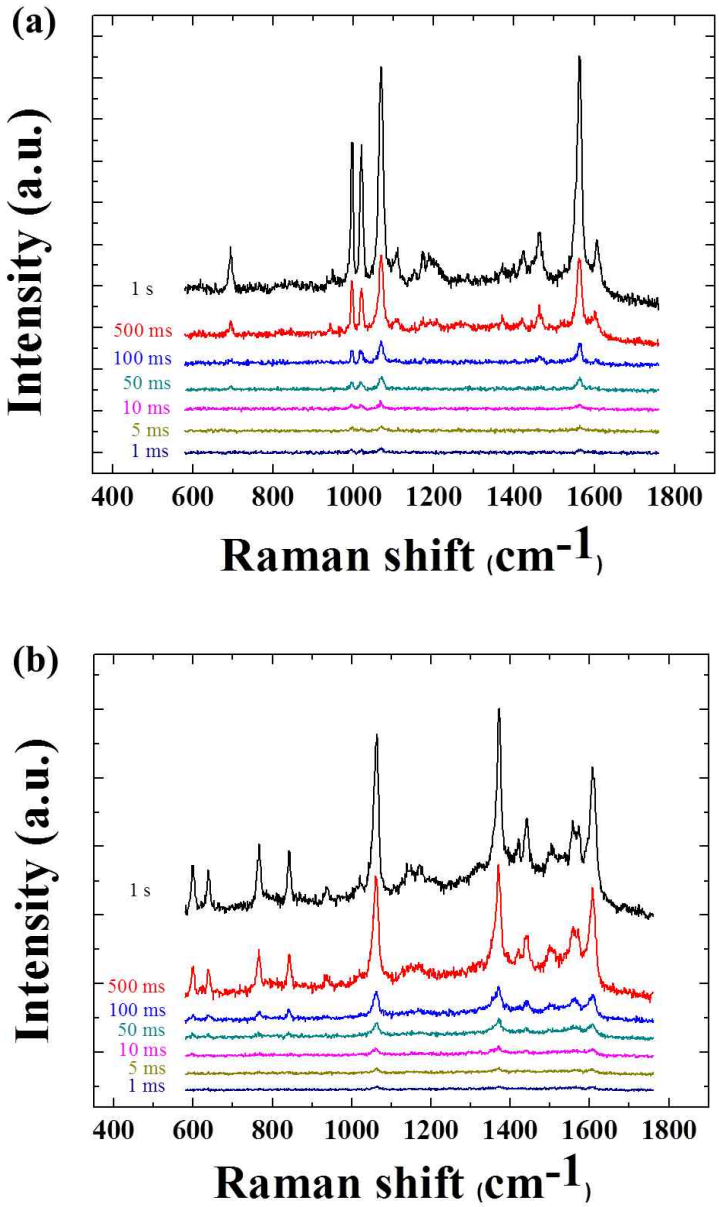

Figure 2-6. The gold bead was reasonably capable of identifying the Raman tag from the spectra with an exposure time that was longer than 1 ms. (a) BT spectra. (b) 2-NT spectra.

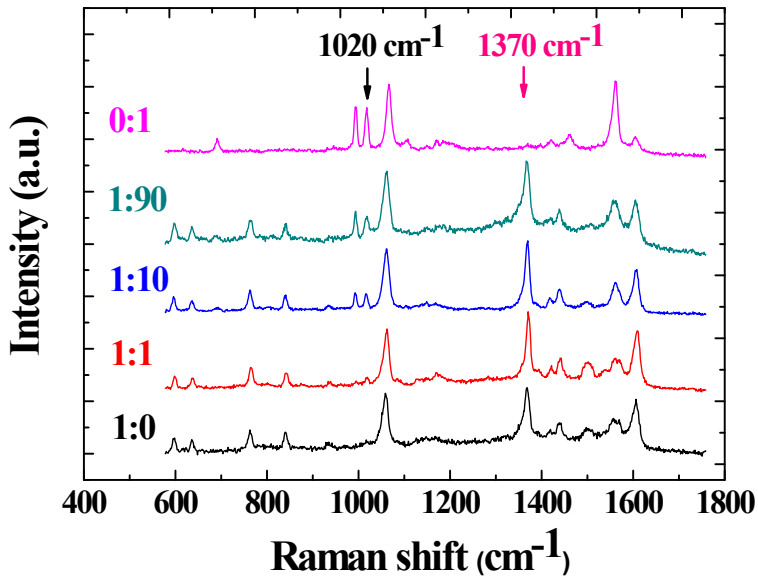

Figure 2-7. SERS spectra of the micro gold beads tagged with mixtures of 2-NT and BT with a series of molar ratios. The 2-NT and BT tags were responsible for the peaks at 1,370 cm^{-1} and 1,020 cm^{-1}, respectively. The relative heights of the peaks at 1,370 cm^{-1} and 1,020 cm^{-1} show the 2-NT:BT ratios of 0:1, 1:90, 1:10, 1:1 and 1:0, respectively. Acquisition time for the SERS measurements was 500 ms.

2.2.2. SERS from Moving Micro Beads in Microfluidic Chip

A few conditions must be fulfilled in order to realize *in situ* SERS decoding of a suspension array on a microfluidic system. First, the beads should be individually addressable using the bead array while travelling in the micro channels on a chip. The beads should neither be too small to be addressed by a laser beam nor too fast to flow along the microchannels. If a microfluidic unit is necessary to allow the beads to precisely pass through the laser spot, the unit must be simple and operate reproducibly. Second, the beads of a suspension array are required to have barcodes, receptors, and a variety of functionalities, e.g. physical or chemical properties for detection, resistivity to nonspecific bonding, magnetism if necessary, etc. Therefore, the desirable surface should allow various chemical modifications using a simple and common methodology. Third, SERS measurements must be completed within a short time because the beads continually move, and thus, the SERS-active surface must be as sensitive as possible. Of course, the SERS characteristic peaks should be identified safely and quickly.

Figures 2-8 (a), (b) and **(c)** show the consecutive SERS spectra for the 2-NT and BT Raman tags and the 2-NT/BT mixture (1:10), respectively, on the micro gold beads flowing in a

microchannel. The individual spectrum (the insets) sampled from the consecutive SERS spectra revealed that the characteristic peaks were clear and their relative intensities successfully represented the fractional ratio of the immobilized Raman tags. The same experiments were carried out using a series of functionalized micro gold beads with mixtures of 2-NT and BT at different ratios (1:1 and 1:90 molar ratios), and the results showed that the ratio of the peak heights quantitatively reflected the fractions of 2-NT and BT on the micro gold beads moving through the microfluidic channels. It should be noted that the micro gold beads were likely to adhere to the glass surface of the microchannel wall and aggregate. The adhesion and aggregation were remarkably reduced by dispersing the micro gold beads in a positive polyelectrolyte, PDADMAC, solution and coating the channel wall with the same polymer.

The careful control of the flow stream was important to precisely focus the excitation laser beam on the functionalized micro gold beads moving through the channel. The sheath flow that was driven by the hydraulic pressure required time to stabilize, and thus, the micro gold beads steadily passed the laser spot one by one. The decoding rate depended not only on the acquisition time of the SERS signals but also on the velocity of the micro gold beads in the channel. If the micro gold beads passed off the laser spot too fast, a

reliable SERS spectrum could not be obtained for identification. On the other hand, very slow moving micro gold beads were not desirable because double decoding could occur for an identical micro gold bead. Therefore, the flow rate must be finely tuned considering both the velocity range of the micro gold beads and the laser exposure time for the consecutive SERS spectra in the microchannels. In this work, the laser exposure time was fixed at 500 ms and the micro gold beads flowed at the optimal velocity which was determined experimentally before decoding. Normally, the flow rate of the micro gold beads ranged from 9 μm/s to 15 μm/s and measured with simple image processing of a movie which was captured with a CCD camera on the microscope. The maximum throughput of the proposed system was 48 objects/min, which was even lower than the decoding capability of the conventional or previously reported methods. However, there is still a lot of potential for improvement for the throughput by virtue of the rapid advancements in laser and surface engineering.

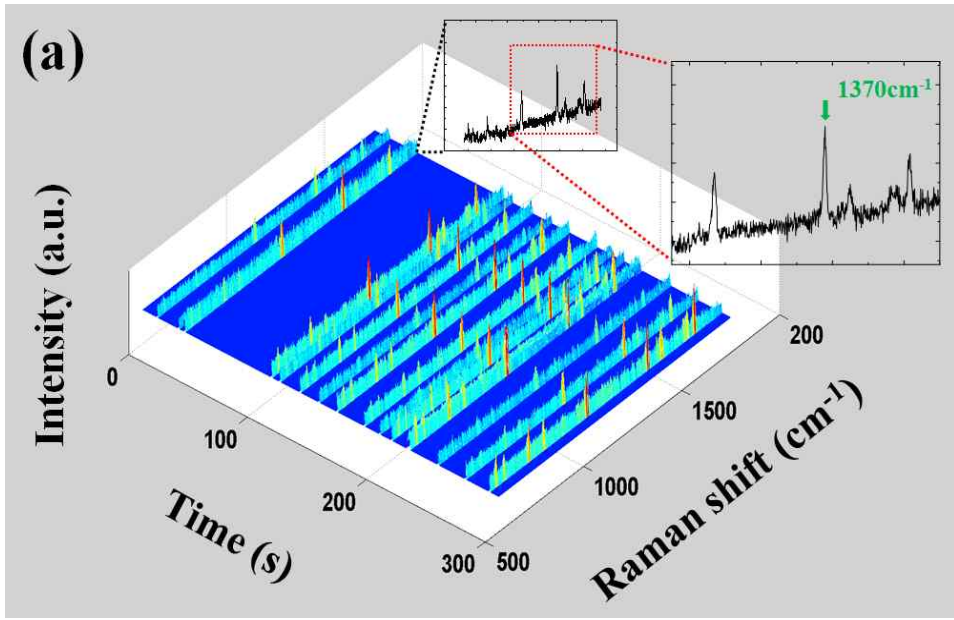
(a)
Intensity (a.u.)
1370cm-1
0
100
200
300
Time (s)
200
1500
1000
500
Raman shift (cm-1)

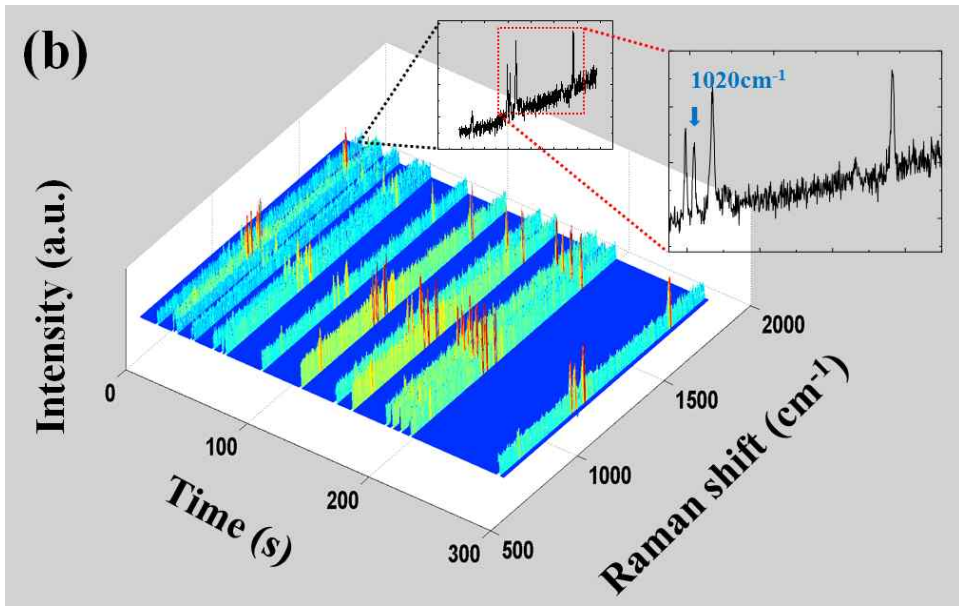
(b)
Intensity (a.u.)
1020cm-1
0
100
200
300
Time (s)
2000
1500
1000
500
Raman shift (cm-1)

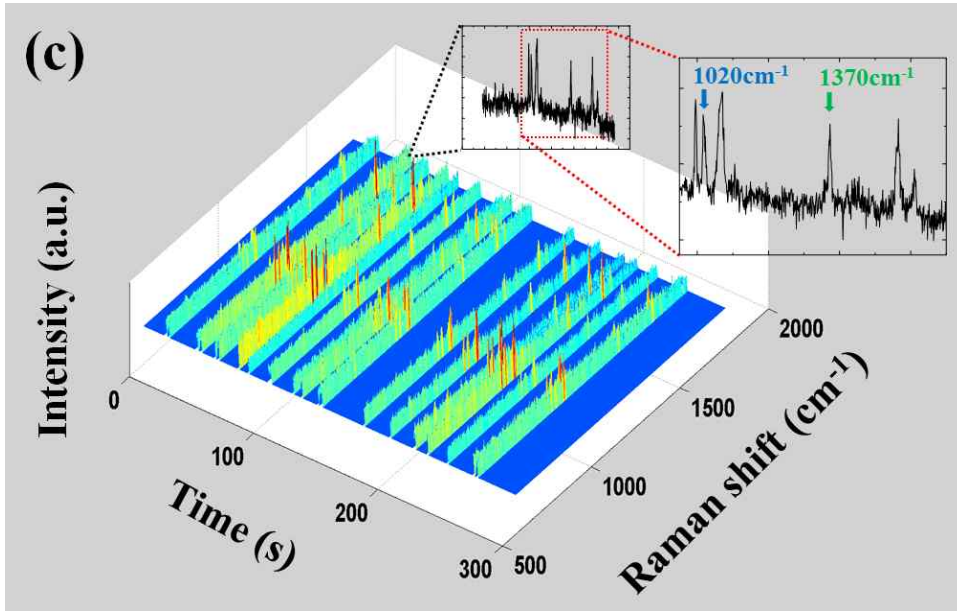

Figure 2-8. Consecutive SERS spectra of the encoded micro gold bead with Raman tags under the fluidic condition. (a), (b) and (c) are the consecutive SERS spectra from the Raman tags of 2-NT, BT and a mixture of 2-NT and BT (1:10), respectively.

2.2.3. SERS Decoding of the Moving Micro Beads

Figure 2-9 shows the histogram of the ratios of the relative intensities of two characteristic peaks for the Raman tagged micro gold beads with various fractional ratios of the Raman tags (2-NT:BT molar ratios of 1:0, 1:1, 1:10, 1:90 and 0:1) in a microfluidic system. The non-overlapping characteristic peaks at 1,020 cm^{-1} for BT (I_1) and 1,370 cm^{-1} for 2-NT (I_2) were chosen, and the normalized intensities I_1 and I_2 were used to decode the moving gold beads. The histogram of the two peaks confirmed the variation in the relative intensities. As a result, the micro gold beads with different ratios of Raman tags were successfully identified in the microfluidic systems. The author calculated the mean and standard deviation of I_1/I_2 (n=10). The results for I_1/I_2 (1:0, 1:1, 1:10, 1:90 and 0:1) were as follows: 0.34 ± 0.07, 0.66 ± 0.07, 1.12 ± 0.08, 1.58 ± 0.24, and 2.47 ± 0.43, respectively.

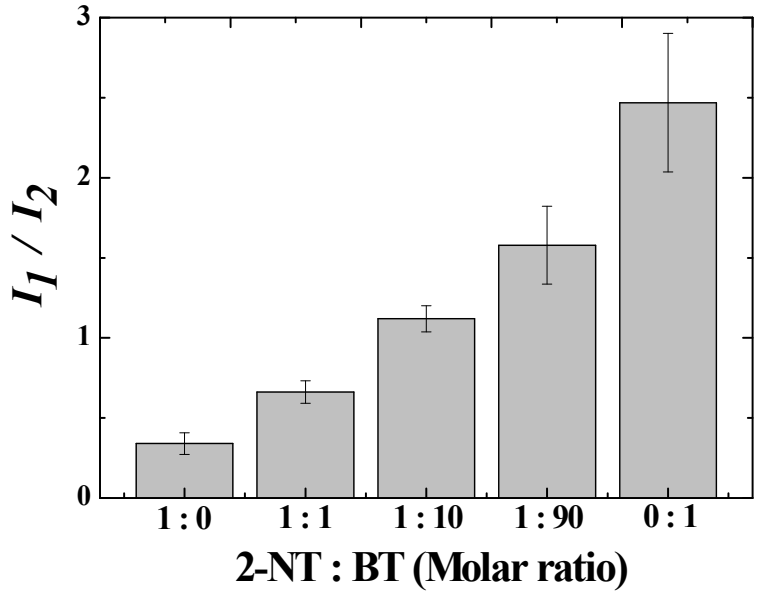

Figure 2-9. Histogram of the characteristic peak ratios of the I_1 (1,020 cm^{-1}) / I_2 (1,370 cm^{-1}) from the SERS spectra in a microfluidic channel. (n = 10)

Chapter 3.

Simultaneous Detection of SERS and Fluorescence Signals Using a Single Excitation Laser Source for Micro Bead-based Analysis

3.1. Methods and Materials

3.1.1. Preparation of Functionalized Micro Beads

Silver micro beads were fabricated with the electroless plating method similar to our previous reports [49, 50]. Briefly, colloidal silver nanoparticles (AgNPs, 2-3 nm in diameter) were attached to amine-terminated poly(methyl methacrylate) beads (PMMA-NH_2, 15 μm in diameter, Bangs Laboratories, Inc) as seed layers. The silver layer was grown by adding AgNP electroless plating solution. The Raman tag (1 mM benzenethiol, BT, Sigma-Aldrich) was dissolved in 1 ml ethanol, and to this solution were added the silver micro beads for 24 h at 4 °C. BT was immobilized on the silver nanoparticles through thiol-silver interactions, whereas the antibody was chemically conjugated with the exposed amine group of the PMMA core. The resulting Raman tagged silver micro beads were centrifuged and washed with DI water several times to remove the excess reagents. Next, the modified silver micro beads with Raman tags were added to a solution containing 100 mM hydrazine hydrate (Sigma-Aldrich) in 50 % methanol for 1 h. For the detection of cardiac troponin I (cTnI) with the immunofluorescence assay, 5 ng of rabbit anti-cTnI antibody were initially incubated with BT-modified and

hydrazine-activated silver micro beads (5 μg) in 0.5 ml of phosphate-buffered saline (PBS) for 1 h at room temperature. The functionalized micro beads were then incubated with 0.4 ng/ml of cTnI in 0.5 ml PBS, followed by incubation of 10 ng of mouse anti-cTnI antibody (GeneTex). The fluorescence was generated with 25 ng/ml of AlexaFluor 610-PE goat anti-mouse IgG (Invitrogen). For the control experiments, either the mouse anti-cTnI antibody or cTnI was removed while keeping everything else the same. Between each reaction step, the resulting beads were rinsed with PBS three times to remove unbound antigens or antibodies. **Figure 3-1** shows a schematic view of the functionalized micro spherical beads.

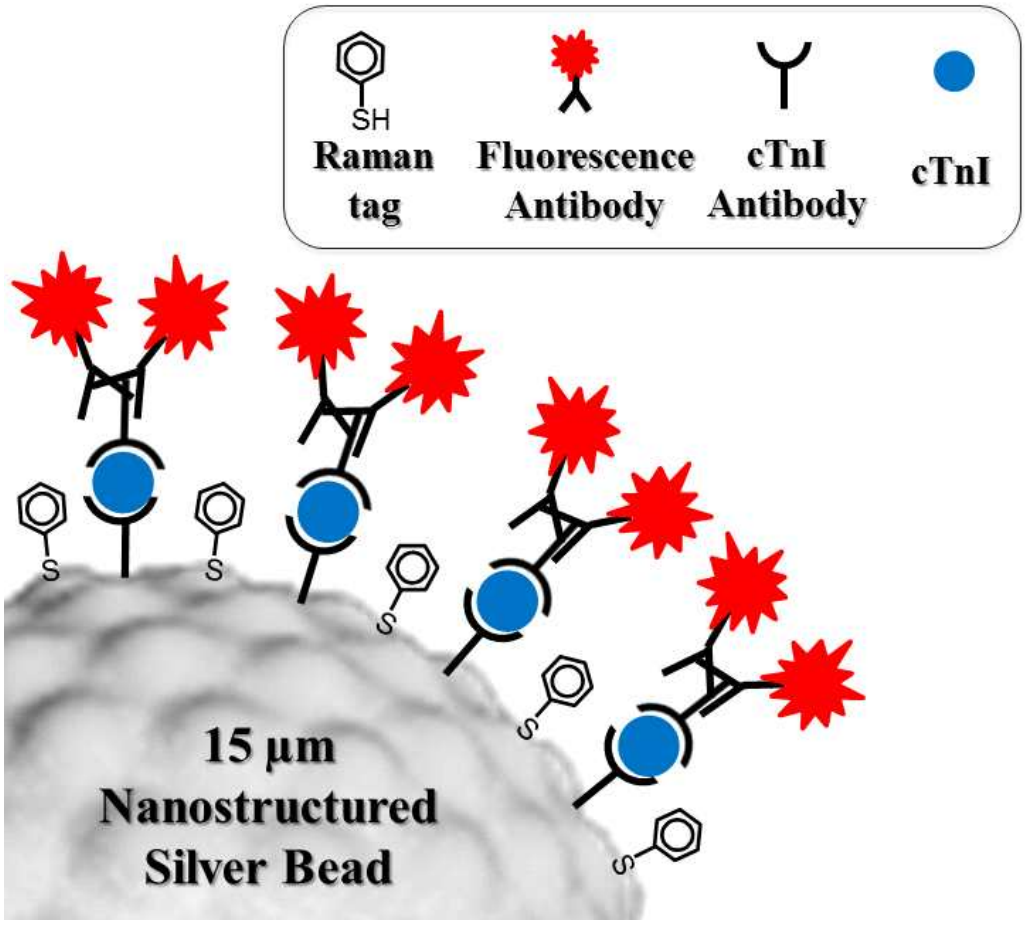

Figure 3-1. Schematic view of the functionalized micro spherical bead. The micro bead has 15 μm PMMA core where the antibody is conjugated with exposed amine groups and has silver nanoparticles on its surface where a Raman tag is chemisorbed (figures not drawn to scale).

3.1.2. Instrumentation for SERS and Fluorescence Measurements

The SERS measurements were performed with a customized micro-Raman spectroscopic system equipped with a microscope. The excitation source was an Argon laser (488 nm, LASOS Lasertechnik GmbH, US) with a maximum output power of 20 mW and a beam diameter of 2 μm. The laser beam was focused through a 50 X objective lens. The SERS was detected using a TE cooled (-50 °C) charge coupled device (CCD) camera (1,024 X 127 pixels, Andor, iDus DV401). The calibration of the spectrometer was achieved with a Raman band of a silicon wafer at 520 cm^{-1} to normalize the peak intensities of the Raman tags. The fluorescence signals from the functionalized beads were detected by a photomultiplier tube (H10721-20, Hamamatsu Photonics Co. Ltd., Japan) equipped with a fluorescence filter (624/40 nm BrightLine® single-band bandpass filter, Semrock, US). For the simultaneous detection of SERS and the fluorescence signals from multiple individual silver micro beads, the beads were spread out on a glass slide and scanned with a laser. The SERS spectrum was windowed at 1,020 cm^{-1} and processed together with the fluorescence signals with the Matlab software (The MathWorks, Inc). The sampling rates of the fluorescence and SERS signals were 10 kHz and 10 Hz, respectively. **Figure 3-2** shows an

overview of the experimental setup for the SERS and fluorescence signal measurements with the functionalized silver micro beads.

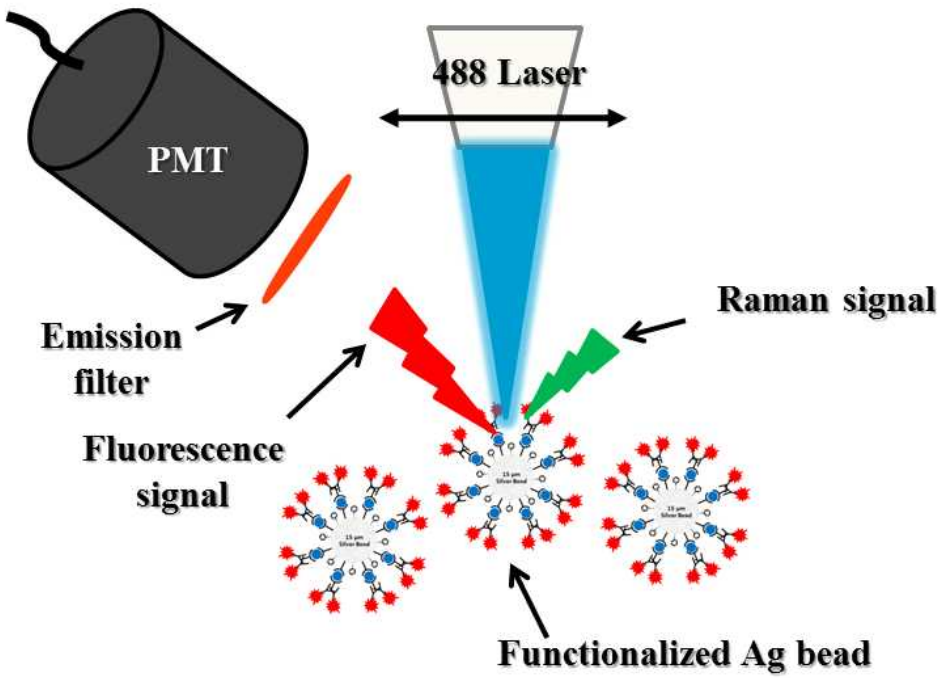

Figure 3-2. Schematic illustrations of experimental set up. The detectors for SERS and fluorescence signals are housed together in a single system. An emission filter (624 nm) is used to select fluorescence signals with PMT while SERS is detected through CCD.

3.2. Results and Discussion

3.2.1. Antibody Response of the Functionalized Micro Beads

Figure 3-3 shows the binding of cTnI, a specific biomarker for myocardial-ischemia, with the antibody on the bead surface. The bead was able to detect 0.4 ng/ml of cTnI, which falls within a clinically relevant detection cut-off [17]. No fluorescence could be detected when cTnI or mouse anti-cTnI antibody was removed in our immunoassay system as a control experiment (**Figure 3-4**). Thus, the fluorescence genuinely originates from an antigen-antibody interaction.

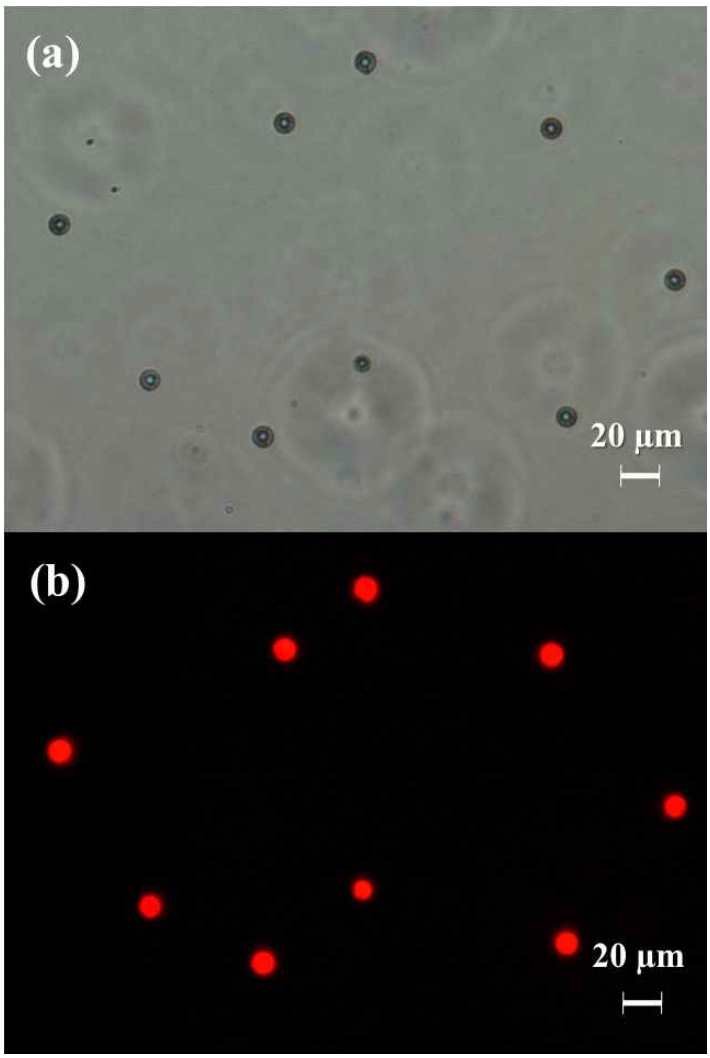

Figure 3-3. Representative microscopy image of functionalized silver micro bead. (a) A light image. (b) A fluorescence image of sandwich immunoassay using 0.4 ng/ml cTnI cardiac marker proteins. Scale bars are 20 μm.

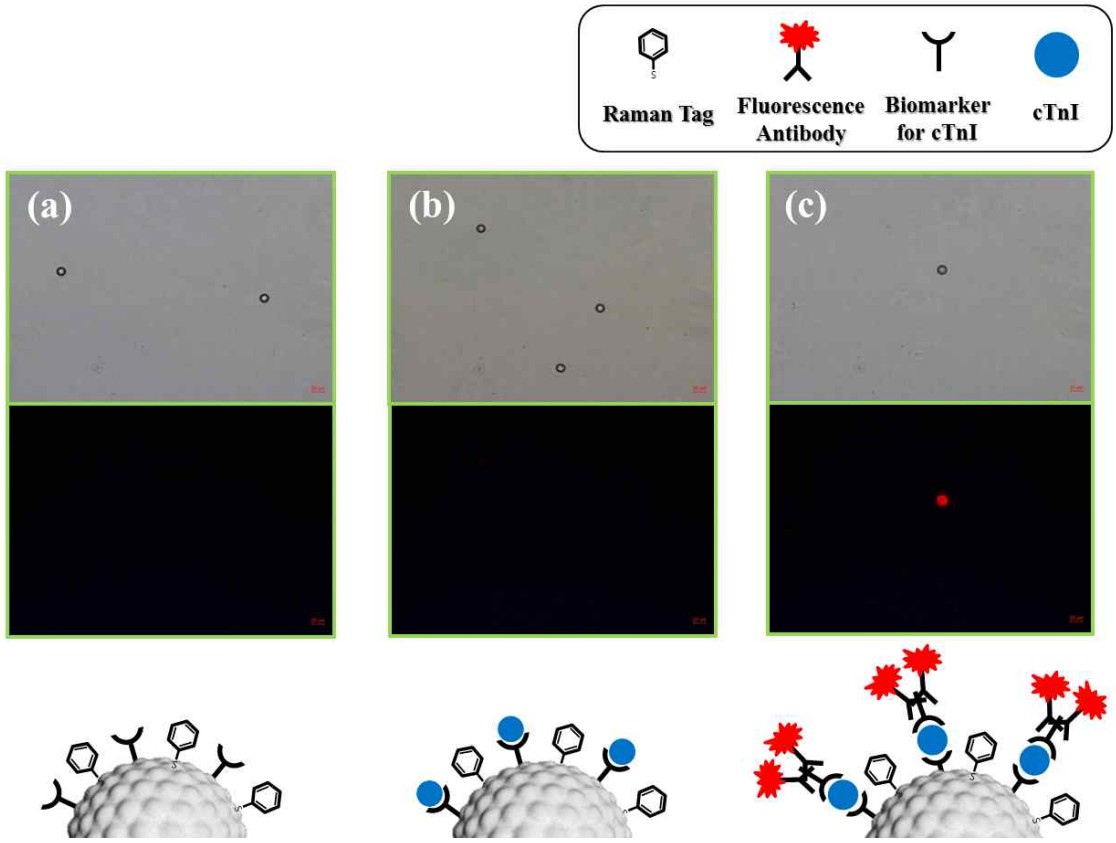

Figure 3-4. Control experiment to evaluate our immunoassay system. No fluorescence could be detected when (a) cTnI or (b) mouse anti-cTnI antibody was removed. (c) Fluorescence could be detected when all of the antigen-antibody response was completed.

3.2.2. Simultaneous Detection of SERS and Fluorescence

The Raman tag is used as identification indices for decoding particular micro beads, while the fluorescence signals provide information about molecular interactions with specific biomarkers. The BT fingerprint peaks at 998, 1,020, 1,073, and 1,567 cm^{-1} clearly stand out from the background. Among them, the two latter peaks typically originate from benzene rings. We chose the 1,020 cm^{-1} peak as a characteristic BT signal for the scanning experiment (vide infra). The detection range of fluorescence signal was designated so that the SERS and fluorescence signals are mutually exclusive to prevent signal overlapping. The typical Raman shift wavenumbers in the SERS spectra, ranging from 600 to 1,900 cm^{-1}, correspond to the wavelengths from 500.72 to 532.87 nm. Therefore, we chose a 624 ± 20 nm filter for fluorescence detection to avoid infringement from the SERS spectra. Of note, a single laser source (488 nm) was used for excitation, while two different detectors, PMT and CCD, were used for the detection of the fluorescence and SERS, respectively.

We then spread the silver micro beads on a glass slide and scanned with the 488 nm laser, simultaneously monitoring the SERS and fluorescence signals. Because the detection ranges of both signals are well separated, simultaneous detection was stably achieved with a

minimum exposure time of 100 ms; the SERS and fluorescence signals exactly coincided throughout the scanning, showing that the silver micro beads carrying the molecular barcode were able to capture the cTnI biomarkers effectively. In our system, while the variation in the SERS intensity does not affect the decoding process, the variation in the absolute fluorescence intensity can be minimized by increasing the number of scanned micro beads to ensure reproducibility. Because the size of our silver micro beads are well suited for microfluidics and the time required for decoding is extremely short, we envision that the integration of our simple barcoding system with microfluidics will produce a high-throughput multiplex assay system.

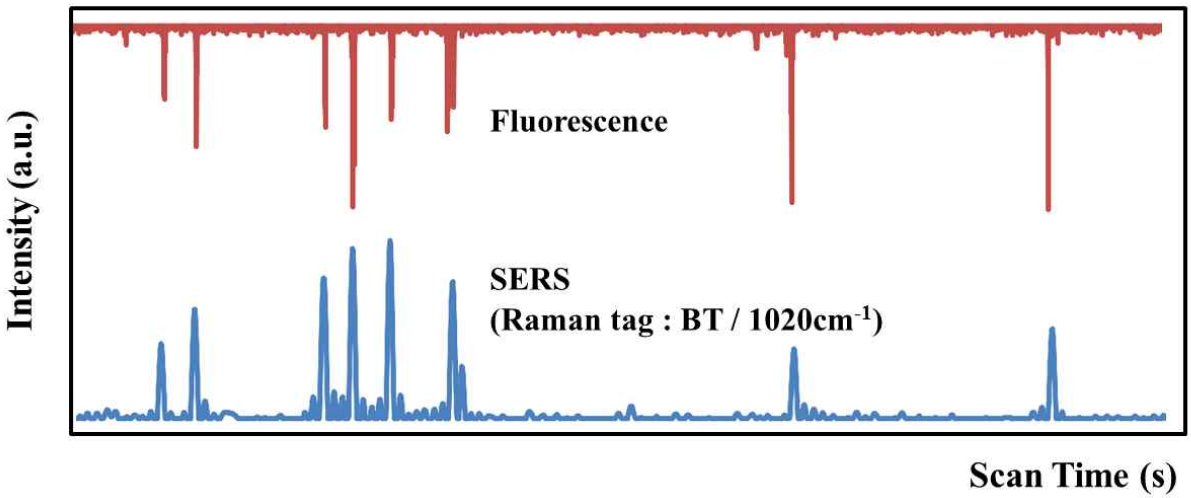

Figure 3-5. Fluorescence (upper) and SERS (lower) signals from a single silver micro bead exactly coincide when simultaneously detected by laser scanning on a glass slide. The peak at 1,020 cm^{-1} was monitored as the representative SERS peak and fluorescence signals were filtered through a 624 ± 20 nm band pass filter.

Chapter 4.

Fluorescence Quantification and SERS Decoding with Micro Beads

4.1. Methods and Materials

4.1.1. Preparation of Modified Micro Beads

The modified micro beads were prepared in the similar manner as the previous process. Briefly, the micro gold beads were fabricated with the electroless plating method [49, 50]. Colloidal gold nanoparticles (AuNPs, 2 to 3 nm in diameter) were synthesized as previously described and attached to amine-terminated PMMA beads (PMMA-NH_2, 15 μm in diameter, Bangs Laboratories, Inc) as seed layers. For the roughened bead structure from the AuNP seed, an Au plating solution composed of $HAuCl_4$ and reducing agents (i.e., formaldehyde and hydroxylamine) was added to the PMMA-NH_2/AuNP solution with vigorous stirring. After all the $HAuCl_4$ was reduced, the solution was centrifuged at 2,000 rpm for 5 min. The rinsing process was repeated several times with deionized (DI) water by centrifuging and then decanting the supernatant. The amounts of added $HAuCl_4$ were adjusted to control the surface topology of the micro gold beads, and the optimal Au loading level was determined by SERS measurements. In this work, 1 mM 2-naphthalenethiol (2-NT, Sigma-Aldrich), 10 mM benzenethiol (BT, Sigma-Aldrich), and a mixture of 2-NT and BT (1:1, 1:10 and 1:90

molar ratios) were employed as Raman tags to functionalize the gold micro beads. The Raman tags were dissolved in ethanol to make 1 mL solutions, and the beads were immersed in the solutions for 24 h at 4 °C. The functionalized micro gold beads were centrifuged and washed with DI water several times to remove the excess reagents. The fluorescence was generated by APC conjugated AlexaFluor 750 antibody (Invitrogen). In this experiment, 0.05 μg, 1 μg, and 10 μg of APC conjugated AlexaFluor 750 antibody were incubated with BT, NT, and the mixture of BT and NT tagged gold beads in 0.5 ml of phosphate-buffered saline (PBS) for 1 h at room temperature. After the reaction step, the resulting beads were rinsed with PBS three times to remove any unbound antigens or antibodies. **Figure 4-1** shows a schematic view of the modified micro spherical beads.

To estimate the enhancement factor, the author used the following equation [82, 83]:

$$EF = \frac{(I_{bead}/N_{bead})}{(I_{bulk}/N_{bulk})}$$

, where I_{bead} and I_{bulk} are the SERS intensities from the BT molecules tagged on the bead surface and the normal Raman intensity of BT in bulk, respectively, and N_{bead} and N_{bulk} are the number of BT

molecules excited by the laser light to obtain the corresponding SERS and normal Raman spectra, respectively. The intensity ratio, I_{bead}/I_{bulk}, is calculated with the 1,024 cm^{-1} Raman shift from the BT molecules with a 633 nm excitation laser for 1 s. Other conditions for the calculation of the enhancement factor were as follow: 110.18 g/mol BT molecules F.W., 1.07 g/cm^3 BT solution density, 2 μm laser spot size, 1.6 μm lens depth of field, and 7.1 x 10^{-10} mol/cm^2 BT concentration on the Au surface. As a result, the enhancement factor from the bead can then be as large as 1.4 x 10^6 (**Figure 4-2**).

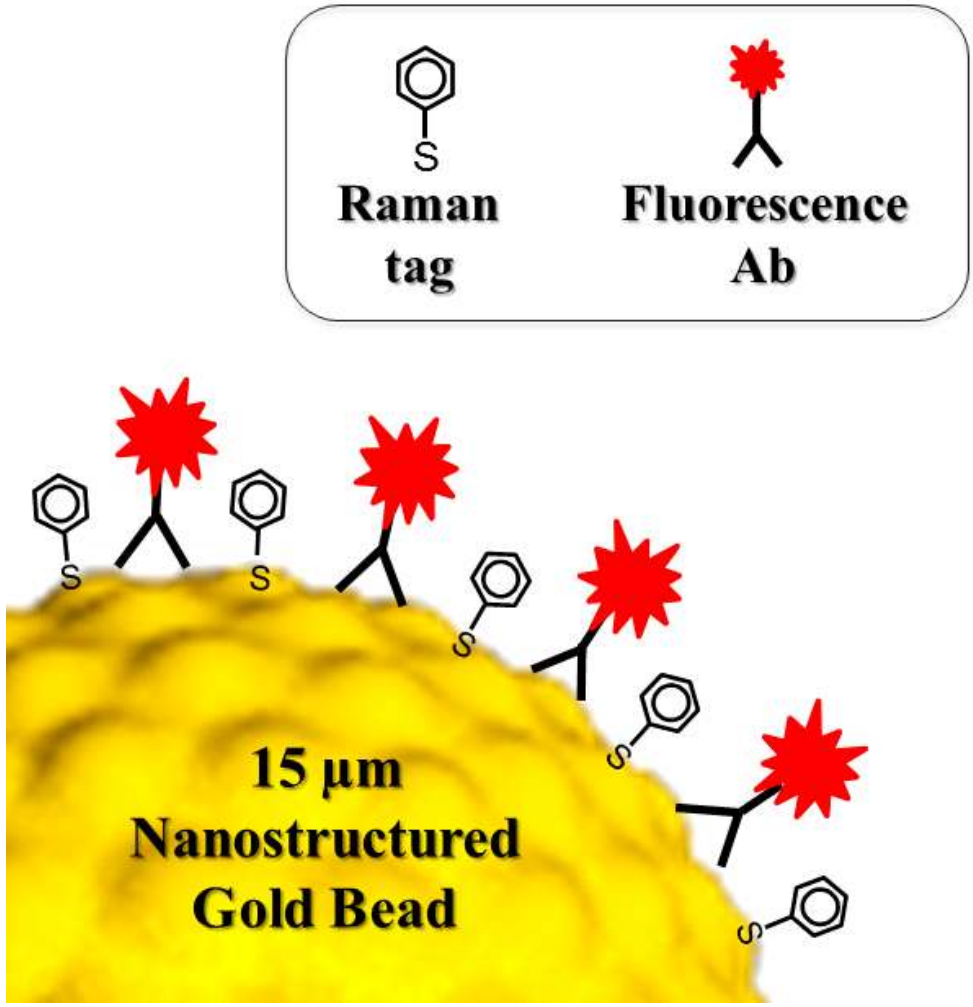

Figure 4-1. Schematic view of the modified micro spherical bead. The micro bead has 15 μm PMMA bead core and fluorescence molecule conjugated antibody is immobilized on its surface and the Raman tag is chemisorbed (figures not drawn to scale).

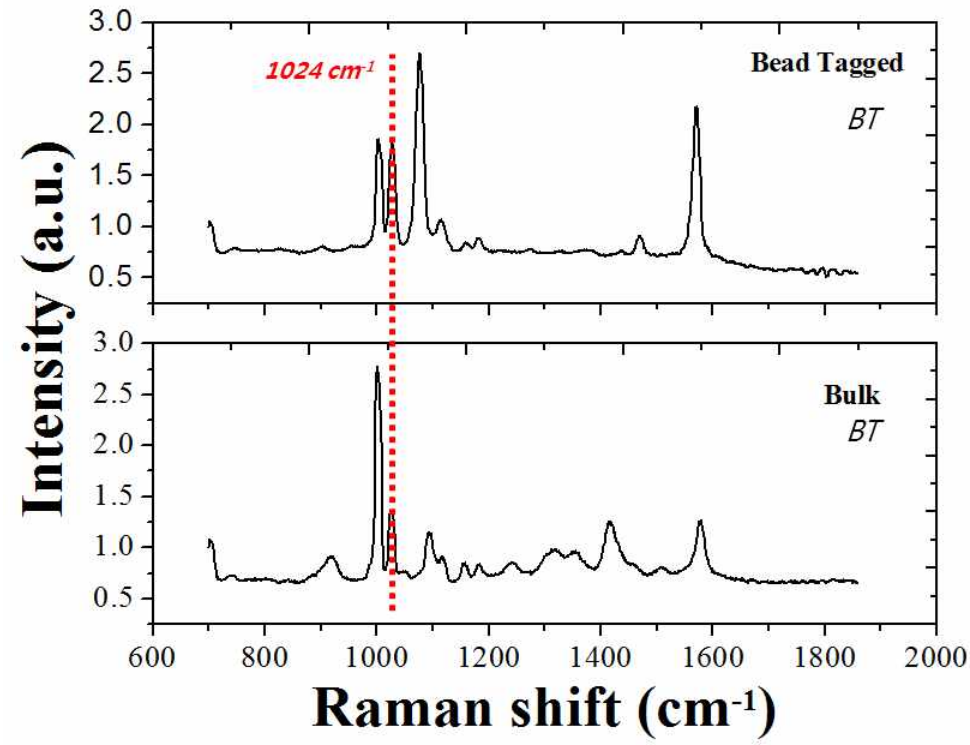

Figure 4-2. Evaluation of the enhancement factor of the micro bead. The enhancement factor can be as large as 1.4 x 10^6, theoretically.

4.1.2. Chip fabrication and Microfluidic system

In order to combine with the other systems, a new version of the microfluidic chip was designed. The new version of the microfluidic chip was fabricated in the same manner with photolithography mentioned in chapter 2. Briefly, a slide glass (Corning, NY, USA) was cleaned in piranha solution (H_2SO_4 : H_2O = 3:1) for 30 min and then baked on a hot plate for drying at 150 °C for 3 min. In order to enhance the adhesion between the glass substrate and the photoresist (PR), hexamethyldisilazane (HMDS) (J.T. Baker, USA) was spin coated onto the glass substrate at 6,000 rpm for 30 s (SC-102, Won Corporation, Korea). The slide glass was then baked on a hot plate at 150 °C for 90 s and cooled to room temperature. The PR (AZ4620, Clariant, Switzerland) was spin coated at 6,000 rpm for 30 s and then soft baked on a hot plate at 100 °C for 90 s. Then, the soft baked slide glass was exposed to ultraviolet (UV) light at 365 nm at a dose of 180 m J cm^{-2} under a photo mask with a mask aligner (MDA-400M, MIDAS system, Korea). The UV exposed PR was developed with a developer (AZ400K, Clariant), and the patterned substrate was hardened by baking it on a hot plate at 150 °C for 15 min to increase the tolerance of the PR to the glass etching solution. With the other side of the slide glass protected, the microchannels

were etched with buffered hydrofluoric acid (NH_4F:HF = 6:1, J.T. Baker) for 40 min at room temperature. The chip was sequentially rinsed with DI water and piranha solution and then sonicated. Holes were drilled as reservoirs on another flat slide glass, and then the etched and the drilled slide glasses were bonded thermally in a melting furnace (CRF-M15, CEBER, Korea) for 24 h. The resulting microfluidic chip was 85 μm wide and 25 μm depth. **Figure 4-3 (a)** shows the fabricated microfluidic glass chip. Bead delivery and sheath are provided by a pressure-driven flow with a syringe pump. For the connection to the pump, NanoPort Assemblies from Upchurch were equipped with a microfluidic chip (**Figure 4-3 (b)**).

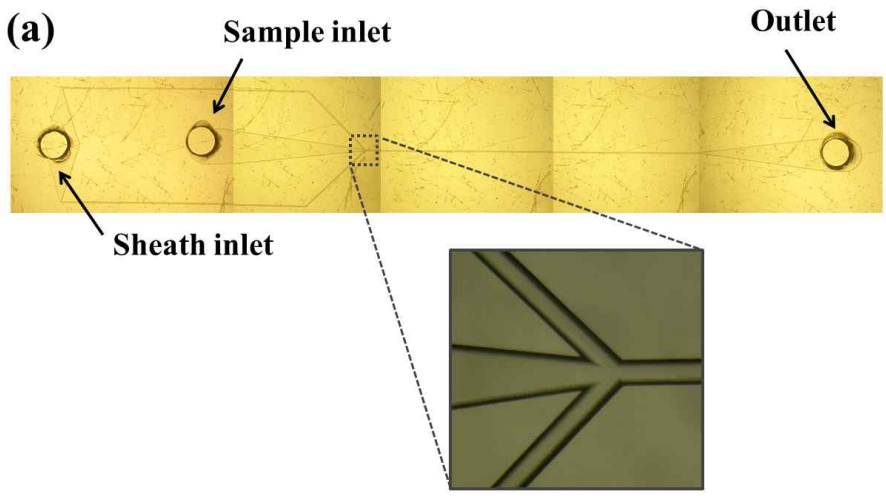

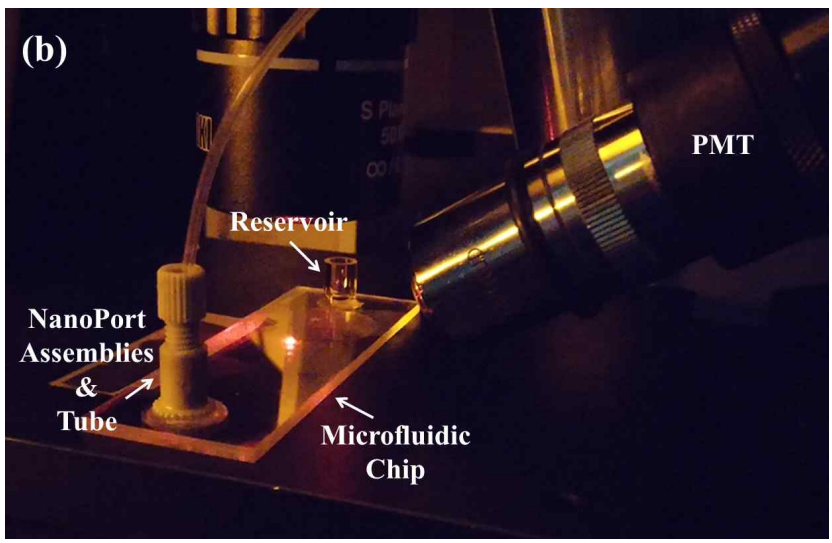

Figure 4-3. (a) The microfluidic glass chip. It was fabricated by standard photolithography and is 85 μm wide and 25 μm depth. (b) The Microfluidic system. Bead delivery and sheath are provided by a pressure-driven flow with a syringe pump. For the connection to the pump, NanoPort Assemblies were equipped with a microfluidic chip.

4.1.3. Instrumentation for SERS and Fluorescence Measurements

The SERS measurements were performed with a customized micro-Raman spectroscopic system equipped with a microscope. The excitation source was a HeNe laser (633 nm, LASOS Lasertechnik GmbH, US) with a maximum output power of 20 mW and a beam diameter of 2 μm. The laser beam was focused through a 50 X objective lens. For a clear SERS signal, optical filters such as a bandpass filter (LL01-633-25, Semrock, US), dichroic filter (LPD01-633RU-25x36x1.1, Semrock, US), and edge filter (LP02-633RE-25, Semrock, US) were equipped to the system. The SERS was detected using a TE cooled (-50 °C) charge coupled device (CCD) camera (1,024 X 127 pixels, Andor, iDus DV401). The calibration of the spectrometer was achieved with the Raman band of a silicon wafer at 520 cm^{-1} to normalize the peak intensities of the Raman tags. The fluorescence signals from the functionalized beads were detected by a photomultiplier tube (H10721-20, Hamamatsu Photonics Co. Ltd., Japan) equipped with a fluorescence filter (750/40 nm BrightLine® single-band bandpass filter, Semrock, US). The fluorescence signal from PMT was transmitted through the DAQ card (National Instrument, US) at 1 kHz sampling rates. The acquired signal was displayed and saved by the self-programmed LabView

software and post processed with the Matlab software. **Figure 4-4** shows an image of the experimental set up.

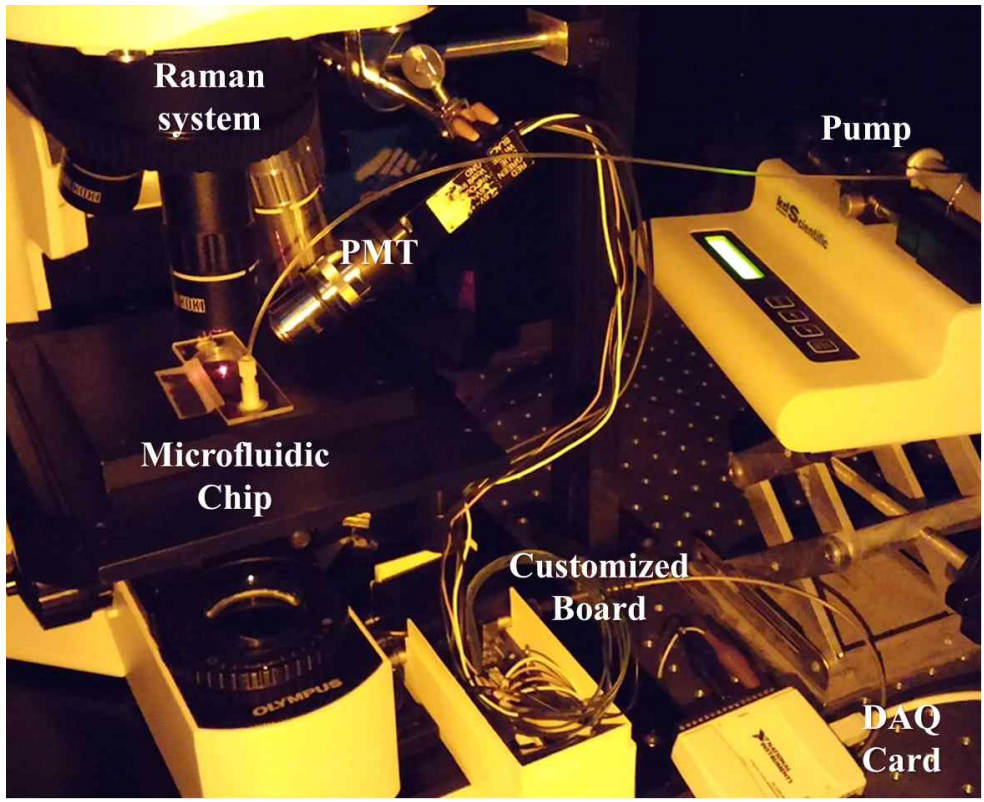

Figure 4-4. An image of the experimental set up. Instrumentations include the Raman system, microfluidic chip, pump system, and data acquisition system.

4.2. Results and Discussion

4.2.1 Optimized Flow Condition for SERS and Fluorescence in a Microfluidic Channel

Because there are differences between the flow determined by the pump and the real flow in the microfluidic channel, the best-fit point has to be found for the system. When the optimal flow was determined, many factors were considered such as the data acquisition time (sampling Hz), cross section area of the microfluidic channel, connection port and capillary, etc. After that, the SERS sampling rates were fixed at 25 Hz and the length of the connection components was set to 30 cm, and only the flow setting of the pump was changed. The change in bead velocity was detected with the imaging CCD operated at 30 frames per second. In this experimental microfluidic system, the optimal pump setting was 30 μL/h (**Figure 4-5**) and the optimal flow rate to detect a reasonable SERS signal from a single bead was 4 ~ 5 points/bead with a fixed data acquisition time (**Figure 4-6**). Theoretical throughput was 102 ~ 138 objects per minute.

To evaluate the performance of the fluorescence system, the author conducted a simple experiment with a fluorescence micro bead

set (bangs lab, US) with an average diameter of 8.31 μm. That standard fluorescence micro bead kit has five different fluorescence intensities of 0.23 %, 1.01 %, 4.60 %, 21.88 %, and 100 %, respectively. (**Figure 4-7**). The fluorescent micro beads with different intensities in 50 μl PBS were loaded into the sample inlet, separately one at a time, and the beads were drawn out at the outlet. The flow rate of the syringe pump (KDS100, KD Scientific) was 30 μl/h. Fluorescence emissions from the beads were detected with PMT and the emission wavelengths were measured at 520 nm. As shown in **Figure 4-8**, the result has good linearity (r^2= 0.9886) and a reasonable error range. The achieved fluorescence system can produce very stable data.

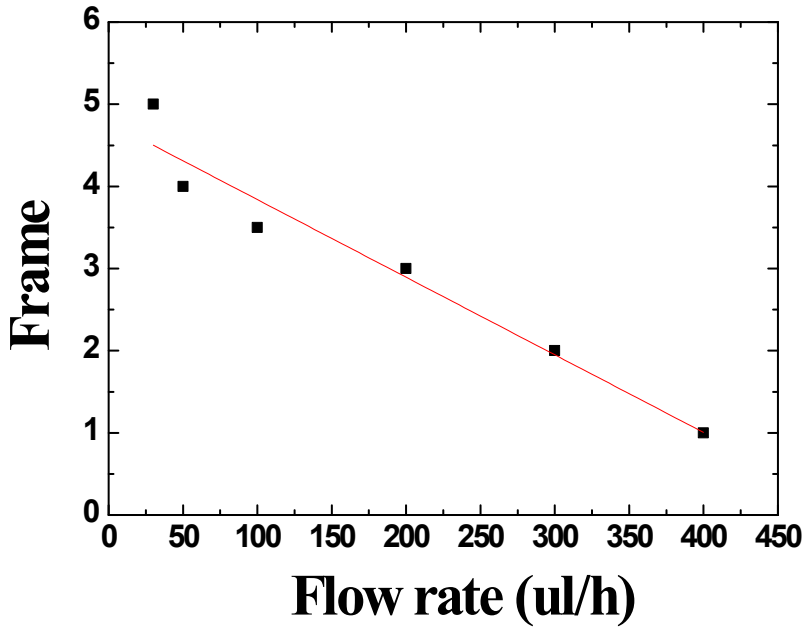

Figure 4-5. Optimized flow condition. The change in bead velocity was detected by imaging CCD operated at 30 frames/second. In this experimental microfluidic system, the optimal pump setting was 30 μL/h.

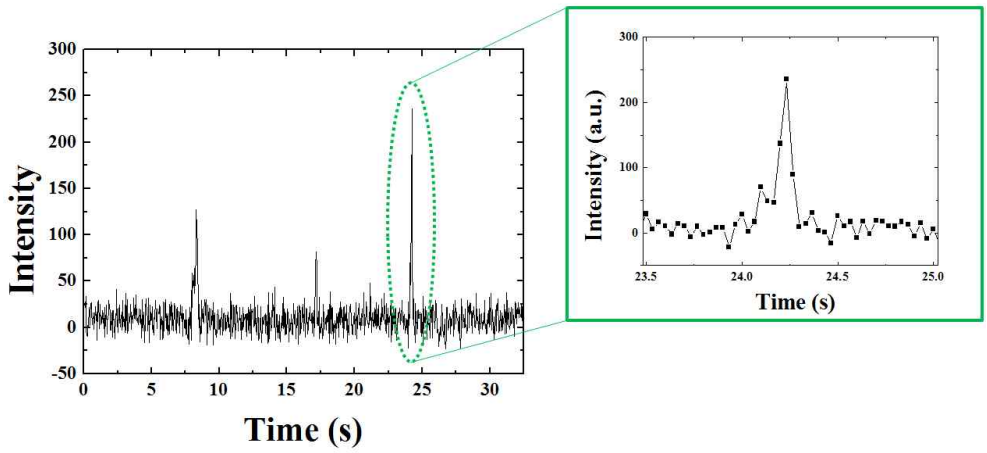

Figure 4-6. Optimized condition for flowing bead control with pump system. Optimal flow rate to detect a reasonable SERS signal from a single bead was 4 ~ 5 points/bead at a fixed data acquisition time.

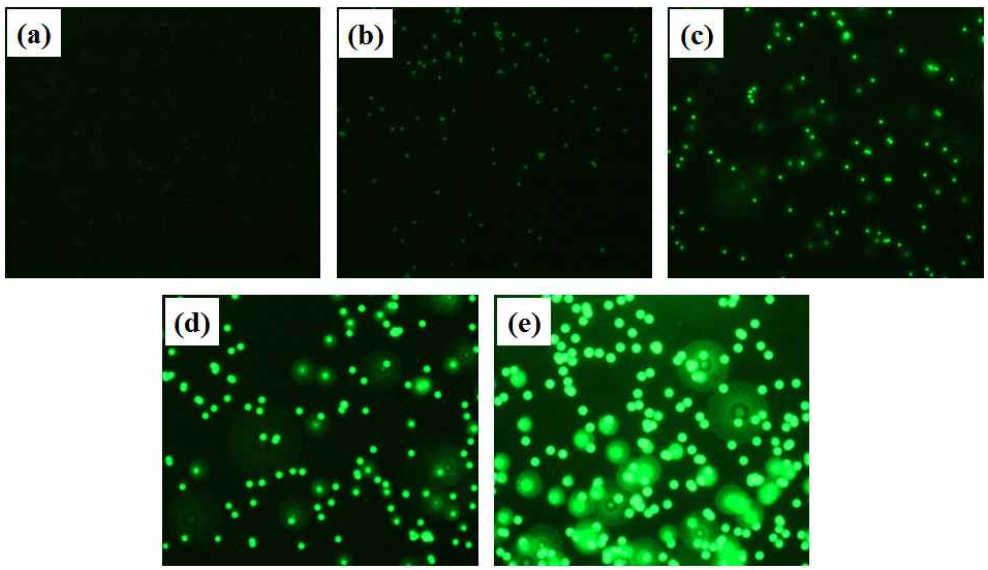

Figure 4-7. Microscopic images of standard fluorescence micro bead. The standard fluorescence micro bead kit from bangs lab with an average diameter of 8.31 μm has five different fluorescence intensities (a) 0.23 %, (b) 1.01 %, (c) 4.60 %, (d) 21.88 %, (e) 100 %.

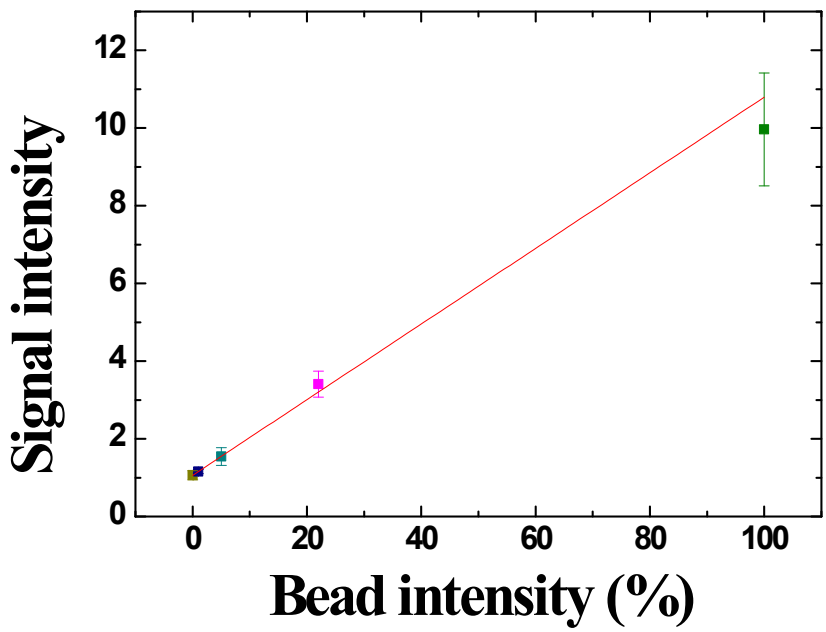

Figure 4-8. Performance evaluation of the fluorescence system. The emission wavelengths were measured at 520 nm by PMT. The results have a good linearity and reasonable error range (r^2= 0.9886).

4.2.2. SERS Decoding and Fluorescence Quantification

SERS and fluorescence signals were obtained simultaneously from a flowing bead in a microfluidic channel. Two independent signals from the bead, the SERS and fluorescence, provide indexing and quantification information, respectively. The mixtures of three different beads, which are encoded with the BT, NT and NT/BT Raman tags and modified with an antibody, were introduced into the microfluidic channel. Decoding with SERS and quantifying with fluorescence, the mixture of beads had clearly separated distributions (Figure 4-9). Figure 4-9 (a) shows histograms of the number of events plotted against the magnitude of the fluorescence from each bead. These fluorescence histograms were found by standard algorithms with the Origin analysis tools. Figure 4-9 (b) shows a scatter plot of the results by the particle transit time plotted against the magnitude of the fluorescence of the modified beads. Although there is some overlap, three different encoded beads can be clearly distinguished. The bead population of the analysis was about three hundreds.

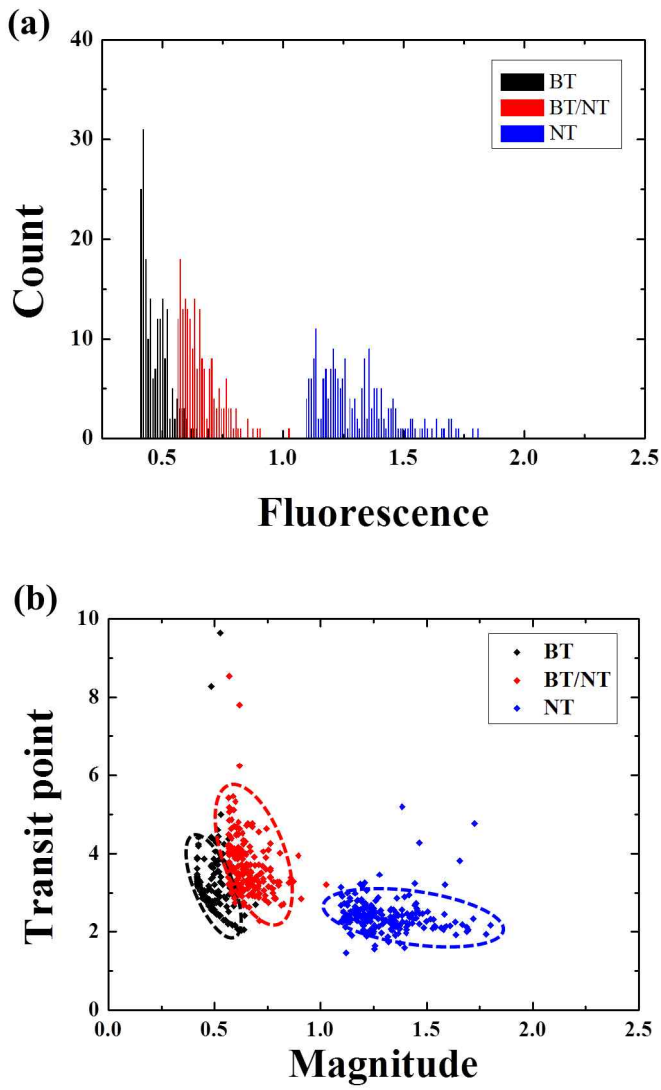

Figure 4-9. (a) Histograms of the number of events plotted against the magnitude of the fluorescence from three different modified beads. (b) Scatter plot of the modified beads delineated by particle transit time against the magnitude of the fluorescence of the modified beads. The bead population is clearly delineated.

Chapter 5.

Conclusion and Prospective

Conclusion and Perspective

The barcoding or indexing strategy for a probe particle is the most important factor for quantifying and classifying the information of a suspension array assay. In this work, the author shows a practical implementation of the SERS decoding strategy for a suspension array assay that existed only in theory and explored the possibility of SERS as a barcoding strategy for a multiplex suspension array as follow: i) consecutive SERS signal acquisition from micro spherical beads moving in microfluidic chip ii) simultaneous detection of SERS and fluorescence signals from micro spherical beads iii) fluorescence quantification and SERS decoding with micro spherical beads for the suspension array.

Chapter 2 presents how the micro gold beads were fabricated using electroless plating on PMMA beads and elegantly optimized to produce the effective SERS signals. The achieved bead produced well-defined SERS spectra even at an extremely short exposure time for a single bead combined with Raman tags such as 2-naphthalenethiol (2-NT) and benzenethiol (BT). The consecutive SERS spectra from a variety of combinations of Raman tags were successfully acquired from the beads ay static and moving conditions. The proposed Raman tagged micro gold bead exhibited potential for

an on-chip microfluidic SERS decoding strategy for a micro suspension array.

Chapter 3 presents the simultaneous detection of SERS and fluorescence signals using a single excitation source which was shown with individually functionalized micro beads that can be applied to array-based multiplex analysis. The author chose the proper beads that could produce well-defined SERS spectra and carefully engineered micro beads with biomarkers. The functionalized micro beads successfully worked dependently, with not only the decoding function of the Raman tags but also with the probing function for analytes. Above all, the author achieved simultaneous detection for SERS and a fluorescence signal, while avoiding signal overlapping between the two by carefully selecting the detection ranges.

In chapter 4, based on the achieved technologies, the author demonstrates the flow cytometer that allows the measurement of fluorescence and SERS signals from a single micro bead in a flow. The flow cytometer includes pump controllable microfluidics and a customized Raman and fluorescence system and it can provide two pieces of independent information which is decoding the results from the encoded Raman tags and quantifying the results from the fluorescence of the modified bead. Through this, the author shows

that the SERS could be a useful decoding strategy for suspension arrays.

Because the SERS decoding strategy has the advantages of narrow spectral features and photostability, it is very attractive as indexing for antibodies or other targeting molecules. However, it is still in the early stage and fluorescence is currently clearly more suitable for indexing. Additional developments in high-speed multispectral detectors, flow cytometric systems, improvements in synthesis methods and surface chemistry will help to realize its full potential in multiplex analysis. The author hopes that this study contributes by providing a facile and efficient methodology for a barcoding strategy for suspension array assays.

Bibliography

[1] Macarron, R.; Banks, M. N.; Bojanic, D.; Burns, D. J.; Cirovic, D. A.; Garyantes, T.; Green, D. V. S.; Hertzberg, R. P.; Janzen, W. P.; Paslay, J. W.; Schopfer, U.; Sittampalam, G. S. Nat Rev Drug Discov 2011, 10, (3), 188-195.

[2] Nolan, J. P.; Mandy, F. Cytometry Part A 2006, 69A, (5), 318-325.

[3] Wilson, R.; Cossins, A. R.; Spiller, D. G. Angewandte Chemie-International Edition 2006, 45, (37), 6104-6117.

[4] Verpoorte, E. Lab Chip 2003, 3, (4), 60n-68n.

[5] Nolan, J. P.; Sklar, L. A. Trends in Biotechnology 2002, 20, (1), 9-12.

[6] Braeckmans, K.; De Smedt, S. C.; Leblans, M.; Pauwels, R.; Demeester, J. Nat Rev Drug Discov 2002, 1, (6), 447-456.

[7] Liu, N.; Gao, Z. X.; Ma, H. W.; Su, P.; Ma, X. H.; Li, X. L.; Ou, G. R. Biosensors & Bioelectronics 2013, 41, 710-716.

[8] Nolan, J. P. Cytometry Part A 2006, 69A, (5), 409-409.

[9] Elshal, M. F.; McCoy, J. P. Methods 2006, 38, (4), 317-323.

[10] Khan, S. S.; Smith, M. S.; Reda, D.; Suffredini, A. F.; McCoy, J. P. Cytom Part B-Clin Cy 2005, 64B, (1), 53-53.

[11] Hildesheim, A.; Ryan, R. L.; Rinehart, E.; Nayak, S.; Wallace, D.; Castle, P. E.; Niwa, S.; Kopp, W. Cancer Epidem Biomar 2002, 11, (11), 1477-1484.

[12] duPont, N. C.; Wang, K. H.; Wadhwa, P. D.; Culhane, J. F.; Nelson, E. L. J Reprod Immunol 2005, 66, (2), 175-191.

[13] Ray, C. A.; Bowsher, R. R.; Smith, W. C.; Devanarayan, V.; Willey, M. B.; Brandt, J. T.; Dean, R. A. J Pharmaceut Biomed 2005, 36, (5), 1037-1044.

[14] Birtwell, S.; Morgan, H. Integr Biol 2009, 1, (5-6), 345-362.

[15] Sukhanova, A.; Nabiev, I. Crit Rev Oncol Hemat 2008, 68, (1), 39-59.

[16] Kawaguchi, H. Prog Polym Sci 2000, 25, (8), 1171-1210.

[17] Kellar, K. L.; Iannone, M. A. Experimental Hematology 2002, 30, (11), 1227-1237.

[18] Hurley, J. D.; Engle, L. J.; Davis, J. T.; Welsh, A. M.; Landers, J. E. Nucleic Acids Research 2004, 32, (22).

[19] Oh, B. K.; Nam, J. M.; Lee, S. W.; Mirkin, C. A. Small 2006, 2, (1), 103-108.

[20] Long, Y.; Zhang, Z. L.; Yan, X. M.; Xing, J. C.; Zhang, K. Y.; Huang, J. X.; Zheng, J. X.; Li, W. Anal Chim Acta 2010, 665, (1), 63-68.

[21] Zhao, Y. J.; Zhao, X. W.; Pei, X. P.; Hua, J.; Zhao, W. J.;

Chen, B. A.; Gu, Z. Z. Anal Chim Acta 2009, 633, (1), 103-108.

[22] Kim, E. Y.; Chang, S. I.; Kang, I. C. Biochip Journal 2007, 1, (2), 102-106.

[23] Gao, X. H.; Nie, S. M. Anal Chem 2004, 76, (8), 2406-2410.

[24] Chan, W. C. W.; Maxwell, D. J.; Gao, X. H.; Bailey, R. E.; Han, M. Y.; Nie, S. M. Curr Opin Biotech 2002, 13, (1), 40-46.

[25] Dejneka, M. J.; Streltsov, A.; Pal, S.; Frutos, A. G.; Powell, C. L.; Yost, K.; Yuen, P. K.; Muller, U.; Lahiri, J. P Natl Acad Sci USA 2003, 100, (2), 389-393.

[26] Nicewarner-Pena, S. R.; Freeman, R. G.; Reiss, B. D.; He, L.; Pena, D. J.; Walton, I. D.; Cromer, R.; Keating, C. D.; Natan, M. J. Science 2001, 294, (5540), 137-141.

[27] Braeckmans, K.; De Smedt, S. C.; Roelant, C.; Leblans, M.; Pauwels, R.; Demeester, J. Nat Mater 2003, 2, (3), 169-173.

[28] Pregibon, D. C.; Toner, M.; Doyle, P. S. Science 2007, 315, (5817), 1393-1396.

[29] Lee, W.; Choi, D.; Kim, J. H.; Koh, W. G. Biomed Microdevices 2008, 10, (6), 813-822.

[30] Vaino, A. R.; Janda, K. D. P Natl Acad Sci USA 2000, 97, (14), 7692-7696.

[31] Nicolaou, K. C.; Xiao, X. Y.; Parandoosh, Z.; Senyei, A.; Nova,

M. P. Angewandte Chemie-International Edition 1995, 34, (20), 2289-2291.

[32] Dunbar, S. A. Clin Chim Acta 2006, 363, (1-2), 71-82.

[33] Houser, B. Archives of Physiology and Biochemistry 2012, 118, (4), 192-196.

[34] Dunbar, S. A.; Jacobson, J. W. Cytometry 2000, 42, (5), 317-318.

[35] de Jager, W.; te Velthuis, H.; Prakken, B. J.; Kuis, W.; Rijkers, G. T. Clin Diagn Lab Immun 2003, 10, (1), 133-139.

[36] Liu, M. Y.; Xydakis, A. M.; Hoogeveen, R. C.; Jones, P. H.; Smith, E. O. B.; Nelson, K. W.; Ballantyne, C. M. Clin Chem 2005, 51, (7), 1102-1109.

[37] Bortolin, S.; Black, M.; Modi, H.; Boszko, I.; Kobler, D.; Fieldhouse, D.; Lopes, E.; Lacroix, J. M.; Grimwood, R.; Wells, P.; Janeczko, R.; Zastawny, R. Clin Chem 2004, 50, (11), 2028-2036.

[38] Kristan, K. A.; Mann, L.; Cox, K.; Treadway, P.; Iversen, P.; Chen, Y. F.; Teicher, B. A. Cancer Chemoth Pharm 2003, 51, (4), 321-327.

[39] Dunbar, S. A.; Vander Zee, C. A.; Oliver, K. G.; Karem, K. L.; Jacobson, J. W. J Microbiol Meth 2003, 53, (2), 245-252.

[40] Nie, S. M.; Emery, S. R. Science 1997, 275, (5303), 1102-1106.

[41] Banholzer, M. J.; Millstone, J. E.; Qin, L. D.; Mirkin, C. A. Chem Soc Rev 2008, 37, (5), 885-897.

[42] Kudelski, A. Talanta 2008, 76, (1), 1-8.

[43] Doering, W. E.; Nie, S. M. J Phys Chem B 2002, 106, (2), 311-317.

[44] Fenniri, H.; Ding, L. H.; Ribbe, A. E.; Zyrianov, Y. J Am Chem Soc 2001, 123, (33), 8151-8152.

[45] Sanles-Sobrido, M.; Exner, W.; Rodriguez-Lorenzo, L.; Rodriguez-Gonzalez, B.; Correa-Duarte, M. A.; Alvarez-Puebla, R. A.; Liz-Marzan, L. M. J Am Chem Soc 2009, 131, (7), 2699-2705.

[46] Sharma, B.; Frontiera, R. R.; Henry, A. I.; Ringe, E.; Van Duyne, R. P. Mater Today 2012, 15, (1-2), 16-25.

[47] Nolan, J. P.; Sebba, D. S. Method Cell Biol 2011, 102, 515-532.

[48] Kim, J. H.; Kang, H.; Kim, S.; Jun, B. H.; Kang, T.; Chae, J.; Jeong, S.; Kim, J.; Jeong, D. H.; Lee, Y. S. Chem Commun 2011, 47, (8), 2306-2308.

[49] Lee, S.; Joo, S.; Park, S.; Kim, S.; Kim, H. C.; Chung, T. D. Electrophoresis 2010, 31, (10), 1623-1629.

[50] Piao, L.; Park, S.; Lee, H. B.; Kim, K.; Kim, J.; Chung, T. D. Anal Chem 2010, 82, (1), 447-451.

[51] Watson, D. A.; Brown, L. O.; Gaskill, D. R.; Naivar, M.;

Graves, S. W.; Doorn, S. K.; Nolan, J. P. Cytometry Part A 2008, 73A, (2), 119-128.

[52] Lee, S. R.; Jeon, C. S.; Hwang, I.; Chung, T. D.; Kim, H. C. J Biomed Nanotechnol 2013, 9, (7), 1241-1244.

[53] Wang, Z. Y.; Zong, S. F.; Li, W.; Wang, C. L.; Xu, S. H.; Chen, H.; Cui, Y. P. J Am Chem Soc 2012, 134, (6), 2993-3000.

[54] Kim, K.; Lee, H. B.; Choi, J. Y.; Shin, K. S. Acs Appl Mater Inter 2011, 3, (2), 324-330.

[55] Yuen, J. M.; Shah, N. C.; Walsh, J. T.; Glucksberg, M. R.; Van Duyne, R. P. Anal Chem 2010, 82, (20), 8382-8385.

[56] Sharma, B.; Cardinal, M. F.; Kleinman, S. L.; Greeneltch, N. G.; Frontiera, R. R.; Blaber, M. G.; Schatz, G. C.; Van Duyne, R. P. Mrs Bull 2013, 38, (8), 615-624.

[57] Haynes, C. L.; McFarland, A. D.; Van Duyne, R. P. Anal Chem 2005, 77, (17), 338A-346A.

[58] Baker, G. A.; Moore, D. S. Anal Bioanal Chem 2005, 382, (8), 1751-1770.

[59] Jehlicka, J.; Vitek, P.; Edwards, H. G. M.; Hargreaves, M. D.; Capoun, T. J. Raman Spectrosc. 2009, 40, (8), 1082-1086.

[60] Haynes, C. L.; Van Duyne, R. P. J Phys Chem B 2003, 107, (30), 7426-7433.

[61] Qin, L.; Banholzer, M. J.; Millstone, J. E.; Mirkin, C. A. Nano Letters 2007, 7, (12), 3849-3853.

[62] Abdelsalam, M. E.; Bartlett, P. N.; Baumberg, J. J.; Cintra, S.; Kelf, T. A.; Russell, A. E. Electrochemistry Communications 2005, 7, (7), 740-744.

[63] Baldelli, S. Chemphyschem 2008, 9, (16), 2291-2298.

[64] Lee, S. J.; Morrill, A. R.; Moskovits, M. J Am Chem Soc 2006, 128, (7), 2200-2201.

[65] Oldenburg, S. J.; Westcott, S. L.; Averitt, R. D.; Halas, N. J. Journal of Chemical Physics 1999, 111, (10), 4729-4735.

[66] Cao, Y. W. C.; Jin, R. C.; Mirkin, C. A. Science 2002, 297, (5586), 1536-1540.

[67] Su, X.; Zhang, J.; Sun, L.; Koo, T. W.; Chan, S.; Sundararajan, N.; Yamakawa, M.; Berlin, A. A. Nano Letters 2005, 5, (1), 49-54.

[68] Jin, R. C.; Cao, Y. C.; Thaxton, C. S.; Mirkin, C. A. Small 2006, 2, (3), 375-380.

[69] Jun, B. H.; Kim, J. H.; Park, H.; Kim, J. S.; Yu, K. N.; Lee, S. M.; Choi, H.; Kwak, S. Y.; Kim, Y. K.; Jeong, D. H.; Cho, M. H.; Lee, Y. S. J Comb Chem 2007, 9, (2), 237-244.

[70] Chon, H.; Lee, S.; Son, S. W.; Oh, C. H.; Choo, J. Anal Chem 2009, 81, (8), 3029-3034.

[71] Huh, Y. S.; Lowe, A. J.; Strickland, A. D.; Batt, C. A.; Erickson, D. J Am Chem Soc 2009, 131, (6), 2208-2213.

[72] Hudson, S. D.; Chumanov, G. Anal Bioanal Chem 2009, 394, (3), 679-686.

[73] Gellner, M.; Kompe, K.; Schlucker, S. Anal Bioanal Chem 2009, 394, (7), 1839-1844.

[74] Sebba, D. S.; Watson, D. A.; Nolan, J. P. ACS Nano 2009, 3, (6), 1477-1484.

[75] Watson, D. A.; Gaskill, D. F.; Brown, L. O.; Doorn, S. K.; Nolan, J. P. Cytometry Part A 2009, 75A, (5), 460-464.

[76] Goddard, G.; Brown, L. O.; Habbersett, R.; Brady, C. I.; Martin, J. C.; Graves, S. W.; Freyer, J. P.; Doorn, S. K. J Am Chem Soc 2010, 132, (17), 6081-6090.

[77] Cecchini, M. P.; Hong, J.; Lim, C.; Choo, J.; Albrecht, T.; Demello, A. J.; Edel, J. B. Anal Chem 2011, 83, (8), 3076-3081.

[78] Pham, T.; Jackson, J. B.; Halas, N. J.; Lee, T. R. Langmuir 2002, 18, (12), 4915-4920.

[79] Joo, S.; Chung, T. D.; Kim, H. C. Sensors and Actuators B-Chemical 2007, 123, (2), 1161-1168.

[80] Kim, K. B.; Chun, H.; Kim, H. C.; Chun, T. D. Electrophoresis 2009, 30, (9), 1464-1469.

[81] Chun, H.; Kim, H. C.; Chung, T. D. Lab Chip 2008, 8, (5),

764-771.

[82] Kim, K.; Kim, K. L.; Lee, H. B.; Shin, K. S. J Phys Chem C 2010, 114, (43), 18679-18685.

[83] Tian, Z. Q.; Ren, B.; Wu, D. Y. J Phys Chem B 2002, 106, (37), 9463-9483.

국 문 초 록

본 논문은 비드를 기반으로 하는 다중분석에서 표면증강라만(SERS)을 활용한 해독전략에 관한 것이다. 탐지입자를 해독하기 위한 바코딩 또는 표지전략은 서스펜션어레이 분석법에서 정보를 정량화하고 분류하기 위한 매우 중요한 요소이다. 본 연구에서는 이론상으로만 논의되었던 서스펜션 분석법을 위한 표면증강라만 해독 전략을 실제적으로 구현하였으며, 다음과 같은 순서로 표면증강 라만 해독 전략의 가능성을 탐구하였다. i) 미세유체 칩 안에서 움직이고 있는 마이크로 비드로부터 연속적인 표면증강라만 신호 획득하기; ii) 기능화한 마이크로 비드로부터 표면증강라만과 형광신호를 동시에 획득하기; iii) 서스펜션 어레이의 마이크로 비드에서 형광정량정보와 표면증강라만 해독정보 획득하기.

첫째, 폴리머(PMMA) 비드에 무전해 도금법을 이용하여 구형의 마이크로 금 비드를 만든 다음, 효과적인 표면증강라만 신호를 내기 위하여 최적화하는 작업을 수행하였다. 2-NT(2-naphthalenethiol)와 BT(benzenethiol)가 라만표지자로 결합된 완성된 비드는 매우 짧은 조사시간에도 불구하고 명확한 표면증강라만 신호를 내었다. 라만표지자들의 다양한 조합으로 기능화 된 비드를 활용하여 멈춰있는 상태와 움직이는 상태 각각에서 연속적인 표면증강라만 신호를 성공적으로 획득할 수 있었다. 이를 통해 연구에서 제안된 라만표지 마이크로 비드가 흐르는 상태에서도 표면증강라만 신호의 해독이 가능함을 보여주었다.

둘째, 다중분석에 활용되기 위한 각각의 기능화 된 마이크로 비드에

서 하나의 여기소스로(excitation source) 표면증강라만 신호와 형광 신호를 동시에 검출하였다. 이를 위해, 저자는 뚜렷한 표면증강라만 신호를 내며 바이오마커로 기능화 된 적절한 마이크로 비드를 구현하였다. 기능화 된 마이크로 비드는 독립적인 라만표지자의 라만부호화(encoding) 뿐만 아니라 분석물의 탐지를 성공적으로 수행하였다. 무엇보다도, 세밀한 신호검출 영역설정을 통하여 표면증강라만과 형광 신호가 겹치지 않고 동시에 획득하는데 성공하였다.

마지막으로, 앞서 성공한 기술들을 바탕으로 흐르고 있는 상태의 마이크로 비드에서 형광과 표면증강라만 신호를 측정할 수 있는 유세포 분석기 (flow cytometer)를 구현하였다. 분석기는 펌프로 조절 가능한 미세유체 시스템, 주문 제작된 라만시스템, 그리고 형광시스템으로 구성되었다. 해당 시스템은 측정된 비드정보를 부호화된 라만 표지자로 해독하고 형광으로 정량하는 독립된 두 가지 정보를 제공한다. 이와 같은 연구를 통하여 표면증강라만이 서스펜션 어레이에 적용 가능한 해독전략임을 보여 주었다.

주요어 : 해독전략, 서스펜션 어레이, 다중분석, 구형 마이크로 비드, 표면증강라만, 형광정량, 흐르는 상태, 미세유체 시스템

학 번 : 2006-20800

감사의 글

대학원 생활을 시작한 게 엊그제 같은데 어느덧 시간이 흘러 학위 과정을 모두 마치고 졸업을 하게 되었습니다. 연구생, 석사과정 그리고 박사과정 시절까지의 모든 시간들은 결코 만만치 않은 것들 이였지만 제 삶에서 중요한 매듭이 또 하나 지어진다고 생각하니 감회가 새롭습니다.

무엇보다, 학위과정 동안 푯대가 되어주신 선생님들께 감사의 말씀을 전하고 싶습니다. 현명한 리더십으로 든든한 버팀목이 되어주신 김희찬 교수님, 항상 묵묵히 지켜봐 주시고 돌봐주셔서 감사합니다. 연구에 대한 열정과 탁월한 학문적 지식으로 연구자의 본을 보여주신 정택동 교수님, 세심하게 지도해주셔서 감사합니다. 의공학이라는 분야에 첫 발을 내딛을 수 있게 해주신 의공학의 대부 민병구 교수님께도 감사드립니다. 제가 비록 빼어난 학생은 못 되었지만, 선생님들의 가르침을 기억하며 부끄럽지 않은 제자로 남기위해 노력 하겠습니다. 또한 부족하기 짝이 없는 학위논문을 심사해주신 최영빈 교수님, 송상훈 교수님, 주세경 교수님께도 감사의 마음을 전합니다.

함께 동고동락했던 의용전자연구실, 전기화학연구실, 인공심장연구실 동료, 선후배님들에게도 이 글을 빌어 아쉬움과 고마움의 마음을 전합니다. 그 동안 함께했던 시간들은 그 무엇과도 바꿀 수 없는 귀한 시간이었고, 앞으로도 제 가슴 속 깊이 기억하겠습니다.

저에게 허락된 가족들에게도 감사의 마음을 전합니다. 모든 것을 바쳐 사랑해주시고 키워주신 나의 아버지, 어머니, 이 논문의 팔 할은 아버

지 어머니께서 밑거름이 돼 주셨기에 가능했습니다. 앞으로도 두 분의 길을 마음깊이 기억하고 지지하겠습니다. 또 다른 모양의 사랑으로 품어 주시는 장인어른, 장모님, 여동생 같은 처제, 감사합니다. 그 누구보다도 나의 아내 조희진에게 고마움을 전합니다. 내가 당신에게 그러한 것처럼, 나에게 있어 당신은 또 다른 나입니다. 사랑하는 사람과 함께함이 얼마나 기쁘고 감사한 일인지 매순간 깨닫게 해주는 당신. 사랑합니다. 나에게 아빠라는 새로운 이름을 선물하고, 하루하루 말로 표현할 수 없는 기쁨을 맛보게 하는 나의 아들 준학, 갓 태어난 너를 품에 안고 고백한 그 다짐을 기억한다. 네 인생의 발판이 될 수 있도록 살아가마.

마지막으로, 저의 모든 것이 하나님 아버지로부터 비롯되었음을 고백합니다. 그 깊은 사랑을 알기에 저는 행복한 사람입니다. 감사합니다.

2014년 2월, 관악에서

이 사 람 올림